Summer 2015

Redescription Of A Specimen Of Pentaceratops (Ornithischia: Ceratopsidae) And Phylogenetic Evaluation Of Five Referred Specimens From The Upper Cretaceous Of New Mexico

Joshua J. Fry
Fort Hays State University, paleofry@gmail.com

REDESCRIPTION OF A SPECIMEN OF *PENTACERATOPS* (ORNITHISCHIA:

CERATOPSIDAE) AND PHYLOGENETIC EVALUATION

OF FIVE REFERRED SPECIMENS FROM THE UPPER

CRETACEOUS OF NEW MEXICO

being

A Thesis Presented to the Graduate Faculty

of the Fort Hays State University in

Partial Fulfillment of the Requirements for

the Degree of Master of Science

by

Joshua J. Fry

B.S., Clarion University of Pennsylvania

Date______________________ Approved_________________________________
Major Professor

Approved_________________________________
Chair, Graduate Council

GRADUATE COMMITTEE APPROVAL

The graduate committee of Joshua J. Fry approves this thesis as meeting partial fulfillment of the requirements for the Degree of Master of Science.

Approved__________________________________
Chair, Graduate Committee

Approved__________________________________
Committee Member

Approved__________________________________
Committee Member

Date______________________

ABSTRACT

Pentaceratops sternbergi is a late Campanian ceratopsian predominately known from the San Juan Basin in New Mexico. Previous specimen descriptions and cladistic analyses are based on partial skulls and composite specimens, which places *Pentaceratops* as an intermediate form between *Chasmosaurus* and *Triceratops*. Recent reports have questioned the taxonomic validity of several referred specimens, leading to taxonomic confusion. To address taxonomic issues, Museum of Northern Arizona specimen MNA V1747 (formerly MNA Pl. 1747) is redescribed and included in the first specimen-based phylogenetic analysis. Additional preparation since the initial description has made available additional skull elements and revealed MNA V1747 to be the most complete *P. sternbergi* skull known. Additionally, this study codes five referred specimens as distinct operational taxonomic units (OTU), then added them to previously published ceratopsian phylogenetic matrices for evaluation. Two consensus trees are produced; a tree comparing the five specimens to the OTU assigned to *P. sternbergi* in recent phylogenetic studies of Ceratopsia and a tree without the *P. sternbergi* OTU. Results indicate that not all specimens included in this analysis can be confidently assigned to *Pentaceratops*, suggesting the possibility of misidentified ceratopsian specimens from the San Juan Basin.

ACKNOWLEDGMENTS

This thesis was made possible through the support and advice of several individuals. A special thanks to Dr. Laura Wilson, my advisor, who had the patience and expertise to propel me through this project, as well as offering her own time to help me improve upon my writing skills. Thanks also to the members of my graduate committee, Dr. Reese Barrick, Dr. Richard Packauskas, and Dr. Robert Sullivan, for reviewing my thesis and making recommendations.

I would like to thank the following individuals for access to specimens used for this study. Access to MNA V1747 is courtesy of the Navajo Nation. Dr. Dave Gillette and his wife Janet Gillette allowed access to the Museum of Northern Arizona collection. They were particularly helpful and accommodating to me on my first solo museum collection trip. I would like to thank Dr. Spencer Lucas for allowing access to the New Mexico Museum of Natural History's collection. He was always helpful and informative when it came to any questions I asked. Finally, I would like to thank Dr. David Burnham for allowing access to the University of Kansas Natural History Museum's collections. He was also very helpful to me, providing specimen information and photos that I did not have at the time.

Additional thanks are given to those who provided me with helpful discussions during the course of this project. I would like to thank Denver Fowler for taking the time to answer several of my questions. His advice provided insight into several parts of this project. I would also like to thank Dr. Spencer Lucas; discussions with him throughout this project provided a great deal of focus for me.

I would also like to give a special thanks to two certain people. First Dr. Robert Sullivan, thank you so much for helping for introducing me to the world of professional paleontology. Before I met him and became his field assistant for two summers, I had little idea how to pursue a career in paleontology. Through his guidance and advice, I was able to find a Master's program to begin my study in paleontology. He is dear friend and I thank him for his contributions. Second and most importantly, I want to thank my mother, Wendy for her constant support and interest in my chosen path. If it wasn't for her reading me every single dinosaur book in the library as a child and taking my siblings and me to museums, I don't think I would be the person I am today. She will never know how much I appreciate her love and support!

TABLE OF CONTENTS

LIST OF TABLES

LIST OF FIGURES

LIST OF APPENDICES

INTRODUCTION

Ceratopsians are well documented from the Upper Cretaceous strata of the American Southwest. The San Juan Basin (SJB) in New Mexico (USA) is one such high yielding area. Gilmore documented the first ceratopsian material from New Mexico in 1916, and the San Juan Basin has produced numerous ceratopsian specimens that have resulted in the recognition of several distinct taxa. One of the most abundant and well-documented of these taxa is *Pentaceratops sternbergi*, a large chasmosaurine ceratopsian. The geographic range of this taxon is relatively restricted, known predominately by over 10 partial to near complete skulls from the San Juan Basin of New Mexico (Osborn, 1923; Wiman, 1930; Lull, 1933; Rowe et al., 1981; Lehman, 1990, 1993, 1998; Dodson et al., 2004; Lucas et al., 2006; Sullivan and Lucas, 2003, 2006; Sampson et al., 2010; Longrich, 2010, 2014). Additionally, a single specimen has been reported from the Upper Cretaceous Williams Fork Formation in Colorado (Diem, 1999; Diem and Archibald, 2000, 2005; Lucas et al., 2006; Longrich, 2014; Sullivan and Lucas, 2006). Specimens referred to the genus range from skull fragments to nearly complete skulls (Osborn, 1923; Wiman, 1930; Lull 1933; Rowe et al., 1981; Lucas et al., 1987; Lehman, 1993, 1998; Sealey et al. 2005).

For this study, the nearly complete skull of MNA V1747 is redescribed to include newly prepared elements. The redescription of this specimen contains characteristics that are not seen in any other *Pentaceratops* specimen and offers a strong baseline for comparison to other ceratopsids and specimens of *Pentaceratops*. Also, a phylogenetic analysis on five previously referred *Pentaceratops* specimens is undertaken to determine the validity of their taxonomic assignment. These five specimens, MNA V1747, NMMNH P-21098 (formerly known as UMN FKK-081), NMMNH P-27468, NMMNH P-50000 (formerly UALP 13342) and KUVP-16100 (formerly UKVP-16100), are first compared to the distinct operational taxonomic unit (OTU) for *P. sternbergi* and the rest of Ceratopsia used in previous phylogenetic analyses. A second phylogenetic is then used that compares the five specimens to the rest of Ceratopsia without the species OTU. The secondary analyses allows for the identification of genuine relationships between the five referred specimens and the rest of Ceratopsia that could otherwise be contain possible bias due to the presences of the Pentaceratops' OTU.

The original description (Osborn, 1923) characterized "*P. sternbergii"* (now *P. sternbergi,* see Lehman 1998, p. 895) by three unique characters: (1) fenestrae of skull elongated not circular, (2) postorbital horns positioned directly over the orbits and curved anteriorly, and (3) epijugals prominent and elongated. However, these characters are no longer considered unique for *P. sternbergi,* as they are expressed in other ceratopsids (Lull, 1933). A second specimen placed in the genus as *P. fenestratus,* was identified based on a unique squamosal fenestra, shorter and more numerous episquamosals, more posterior position of supraorbital horns relative to orbits, shorter epijugals, and a longer posteriorly directed nasal horn (Wiman, 1930; Lull, 1933). These characters are now attributed to being either pathologies or examples of intraspecific variation based upon comparisons to other well-known chasmosaurines (Mateer, 1981; Lehman, 1989, 1990, 1993). *P. fenestratus* has been synonymized with *P. sternbergi* (Lehman, 1993), resulting in a monospecific genus.

A skull collected by the Museum of Northern Arizona (MNA V1747, formerly MNA Pl. 1747) in 1977 provided new information on the parietal, which was absent in all other known specimens at that point (Rowe et al., 1981). As a result, Rowe et al's description focused primarily on the orientation of parietal epoccipitals and the squamosal-parietal frill (Fig. 1). Unfortunately, the specimen was not fully prepared and was still in its field jacket at the time of its original description so only the posterior side of the skull was exposed and several cranial elements were obscured. The specimen has since been fully prepared, but not fully studied until now.

Recent published works (Sullivan et al. 2005; Jasinski et al. 2011; Sullivan and Lucas, 2015, in press) have investigated the taxonomic validity of specimens NMMNH P-25084 (formerly UMN FKK-035) and NMMNH P-21098 that are referred to *Pentaceratops* by Lehman (1993). These specimens are incomplete skull elements found in a rock stratum than that of other *Pentaceratops* specimens. NMMNH P-21098 is included within this study due to its exemption in Jasinski et al. (2011) and Sullivan and Lucas (2015, in press). Those studies have suggested that no ceratopsian material within the De-Na-Zin can be referred to *Pentaceratops*. However, no cladistical data has been reported to support this claim.

A number of phylogenetic analyses of Chasmosaurinae have been published in recent years (Sampson et al. 2010; Mallon et al. 2011, 2014; Wick and Lehman 2013) (Fig. 2). However, no analysis has been performed on individual specimens assigned to *Pentaceratops* to confirm their assignment. Additionally, the OTU for the genus used in these studies is a composite character matrix that incorporates data from the holotype and four other *P. sternbergi* specimens. This conglomerate complex does not state which *P. sternbergi* character comes from which referenced specimen. The original matrix authors (Sampson et al. 2010) make the assumption that all the specimens chosen for this *P. sternbergi* OTU are all of the same species.

The five specimens in this study are individually coded and subjected to a specimen based phylogenetic analysis to determine taxonomic assignment. Three of those specimens, MNA V1747, NMMNH P-27468 and NMMNH P-50000 are three of the five referred specimens used to define the OTU for *P. sternbergi* in recent matrices (Sampson et al. 2010; Mallon et al., 2011, 2014; Wick and Lehman 2013). This study evaluates the assumption made by Sampson et al. (2010) that those three specimens are *P. sternbergi*.

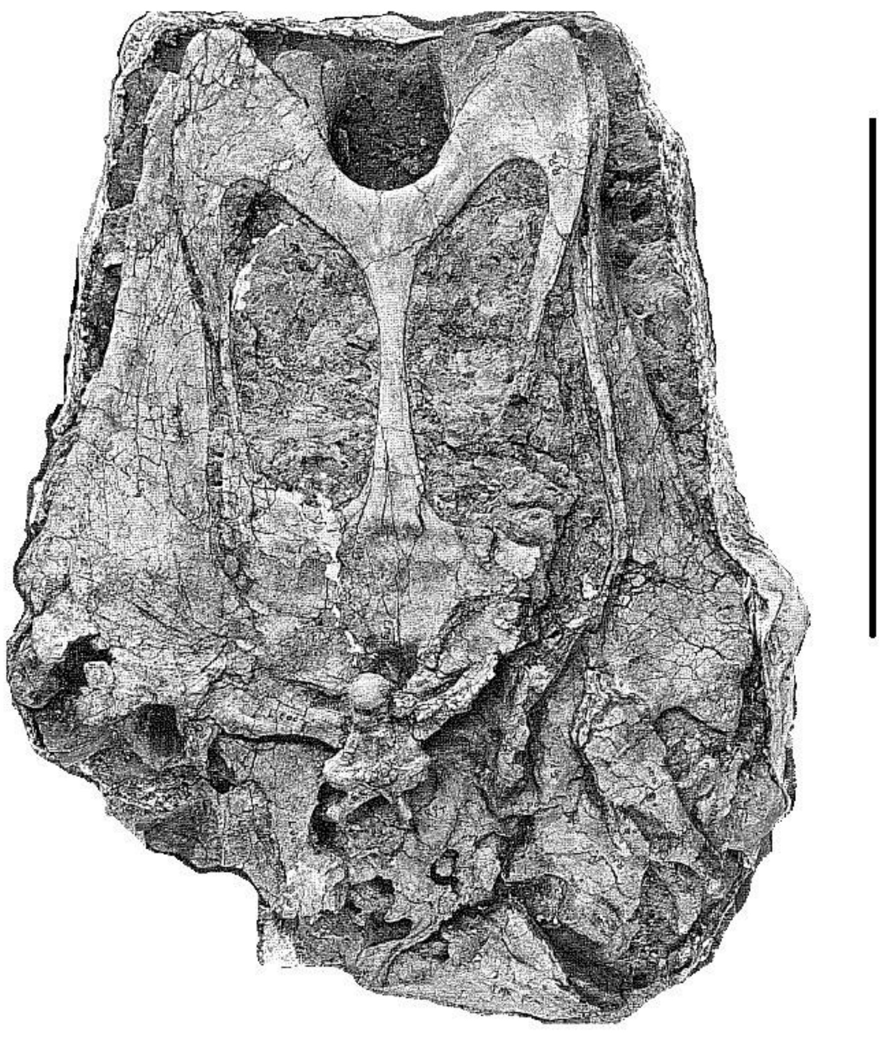

Fig. 1. Posterior view of MNA V1747 in field jacket. Modified from Rowe et al. (1981). Scale bar represents one meter.

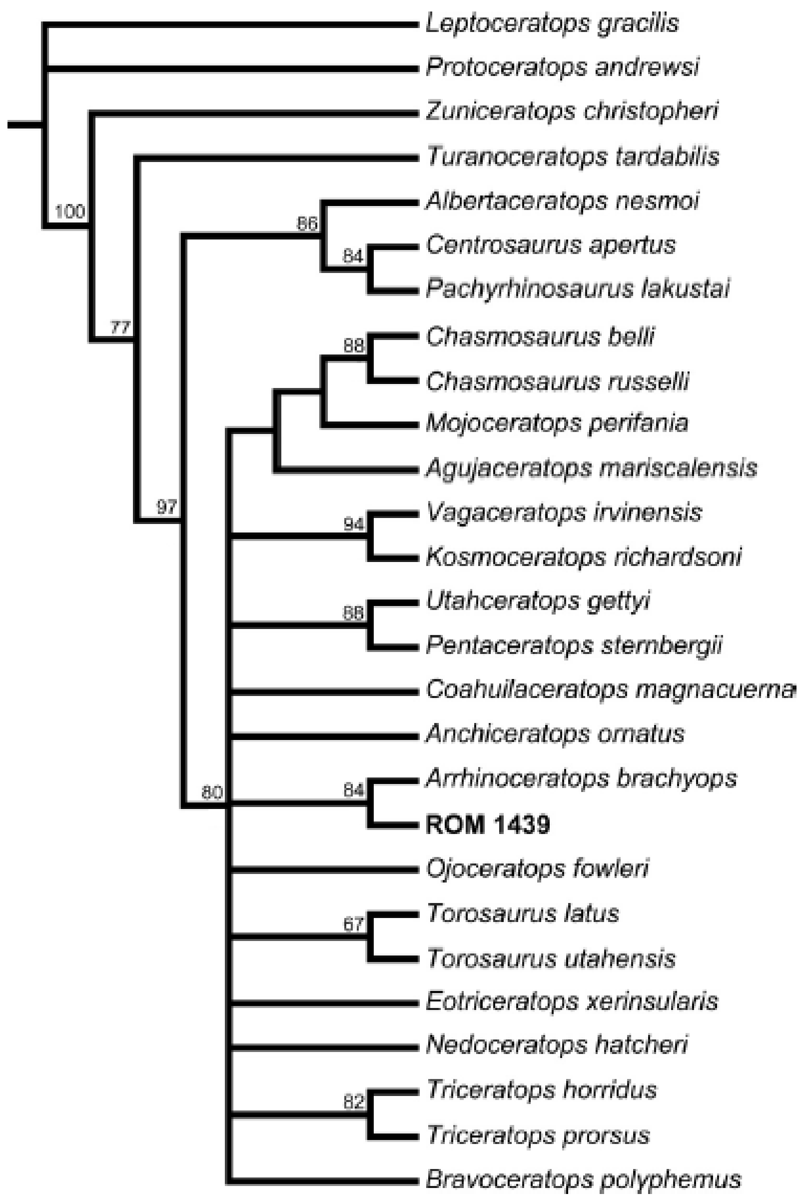

Fig. 2. Strict consensus tree incorporating (Royal Ontario Museum) ROM 1439 (in bold). Frequency above 0.5 shown. TL of 338 steps, CI of 0.527, and RI of 0.634. Modified from Mallon et al. (2014)

Institution Abbreviations

AMNH, American Museum of Natural History, New York City; **KUVP** (formerly known as UKVP), University of Kansas Natural History Museum, Lawrence; **MNA**, Museum of Northern Arizona, Flagstaff; **ONMH**, Oklahoma Museum of Natural History, Norman; **NMMNH** (formerly known as UMN), New Mexico Museum of Natural History, Albuquerque; **PMU**, Museum of Evolution Uppsala University, Sweden; **UALP**, University of Arizona Laboratory of Paleontology, Tucson.

Anatomical Abbreviations

ang, angular; **angp**, angular process; **bo**, basioccipital; **bot**, basioccipital tuber; **bpt**, basipterygoid process; **cp**, coronoid process of dentary; **d**, dentary; **ej**, epijugal; **eoc**, exoccipital; **ept**, pterygoid eminence; **ex nas**, external naris; **f**, frontal; **isf**, interseptal foramen; **ju**, jugal; **lac**, lacrimal; **m**, maxilla; **mf**, mandibular fossa; **nas**, nasal; **nh**, nasal horn; **nst**, nasal strut; **nuc**, nutrient channel; **o**, orbit; **oc**, occipital condyle; **os**, occlusal surface; **P1-3**, epiparietals; **pa**, parietal; **paf**, parietal fenestra; **pd**, predentary; **pf**, postfrontal; **pg**, pterygoid groove; **pm**, premaxilla; **pmf**, premaxillary fossa; **pmp**, premaxilla process; **po**, postorbital**; prf**, prefrontal; **q**, quadrate; **qj**, quadratojugal; **r**, rostral bone; **sang**, surangular; **soh**, supraorbital horncores; **sq**, squamosal; **Sq1-5**, episquamosals; **sqp**, squamosal process.

MATERIAL AND METHODS

Material

Several specimens consisting of partial frills to complete skulls have been referred to *Pentaceratops*. Five of those specimens are used in this study: MNA V1747 (Rowe et al. 1981; Lehman, 1990, 1993; Sampson et al. 2010; Mallon et al., 2011, 2014; Wick and Lehman 2013), NMMNH P21098 (Lucas et al. 1987; Lehman 1993), NMMNH P27468 (Sealey et al. 2005; Sampson et al. 2010; Mallon et al., 2011, 2014; Wick and Lehman 2013), NMMNH P50000 (Rowe et al. 1981; Lehman, 1990, 1993; Sampson et al. 2010; Mallon et al., 2011, 2014; Wick and Lehman 2013) and KUVP-16100 (Rowe et al. 1981; Lehman, 1990, 1993).

MNA V1747 consists of a nearly complete disarticulated skull, including mostly complete lower jaws, several incomplete cervical ribs, vertebrae thoracic ribs, and one complete pubis. Though the exact locality is in question, MNA V1747 is plotted in the upper Fruitland, following Rowe et al., (1981).

NMMNH P-21098 is a partially complete skull consisting of incomplete squamosals with fused rectangular episquamosals, a right supraorbital horncore and a partial orbit, a predentary, a single well preserved vertebra, a single disarticulated surangular, and a well preserved scapula with fused coracoid. Originally described as being from the Naashoibito Member of the Ojo Alamo Formation (Lucas et al. 1987), NMMNH P-21098 was relocated to the De-Na-Zin Member of the Kirtland Formation by Lehman (1993) (Fig.3). Past studies note that ceratopsian specimens from the De-Na-Zin are not referable to *Pentaceratops* (Jasinski et al. 2011; Sullivan and Lucas, 2015, and in press). NMMNH P-21098 is only recently mentioned explicitly in Sullivan et al. (2005), which only confirms its position in the De-Na-Zin Member. For this study, NMMNH P-21098's stratigraphic position is also confirmed, while its taxonomic assignment is tested within two phylogenetic analyses.

NMMNH P-27468 is a partial skull with a nearly complete parietal, that also includes a partial right squamosal, a quadrate, a nearly complete jugal with fused epijugal, a nearly complete vertebra, and incomplete ribs with associated bone fragments. This specimen was assigned to *P. sternbergi* in an abstract by Sealey et al. (2005) and is found within middle section of the Hunter Wash Member of the Kirtland Formation (Fig. 3).

NMMNH P-50000 is a partial skull that is medio-laterally compressed; the posterior half of the squamosals and the entire parietal are absent, and the right supraorbital horncore is missing, but a cast of the original horncore exists. NMMNH P-50000 is stratigraphically located in the upper sediments of the Hunter Wash Member (Fig. 3).

KUVP-16100 consists of a nearly complete fragmented skull with the anterior portion partially missing. Missing elements include the right jugal and epijugal, anterior portion of the nasals and nasal horncore, the premaxillae, rostrum, and lower jaws. KUVP-16100 is located in the Fossil Forest Member of the Upper Fruitland Formation (Fig. 3).

Several specimens are excluded from this study due to incompleteness or lack of accessibility. AMNH 1624, AMNH 1622, and OMNH 10165 are all incomplete skulls that lack frills, and AMNH 1625 is the posterior half of a single squamosal with fused epoccipitals. Most of these specimens' localities are unable to be verified. Additionally, though OMNH 10165 originally assigned to *Pentaceratops* (Lehman, 1998), it has since been assigned to its own genus (Longrich. 2010). Although Wick and Lehman (2013) overlooked this assignment, the new genus has been rejected and synonymized with *P. sternbergi* by Sullivan and Lucas (2015, in press). PMU 24922 (formerly PMU. R200) is excluded due to its extreme taphonomic distortion.

As stated above, the OTU for the taxon *P. sternbergi* consists of characters of the holotype, AMNH 6324, with AMNH 1624, MNA V1747, NMMNH P27468, and NMMNH P50000 as reference material for the character matrix (Appendix 1). No distinction has been made in previous studies to which characters of the OTU come from which of the five specimens. MNA V1747, NMMNH P27468, and NMMNH P50000 are included based upon their relative completeness compared to the excluded fourth specimen, AMNH 1624. AMNH 6324 is a nearly complete skull with only the left lateral edge of the frill preserved, but was not available to be individually coded by the author in for this study.

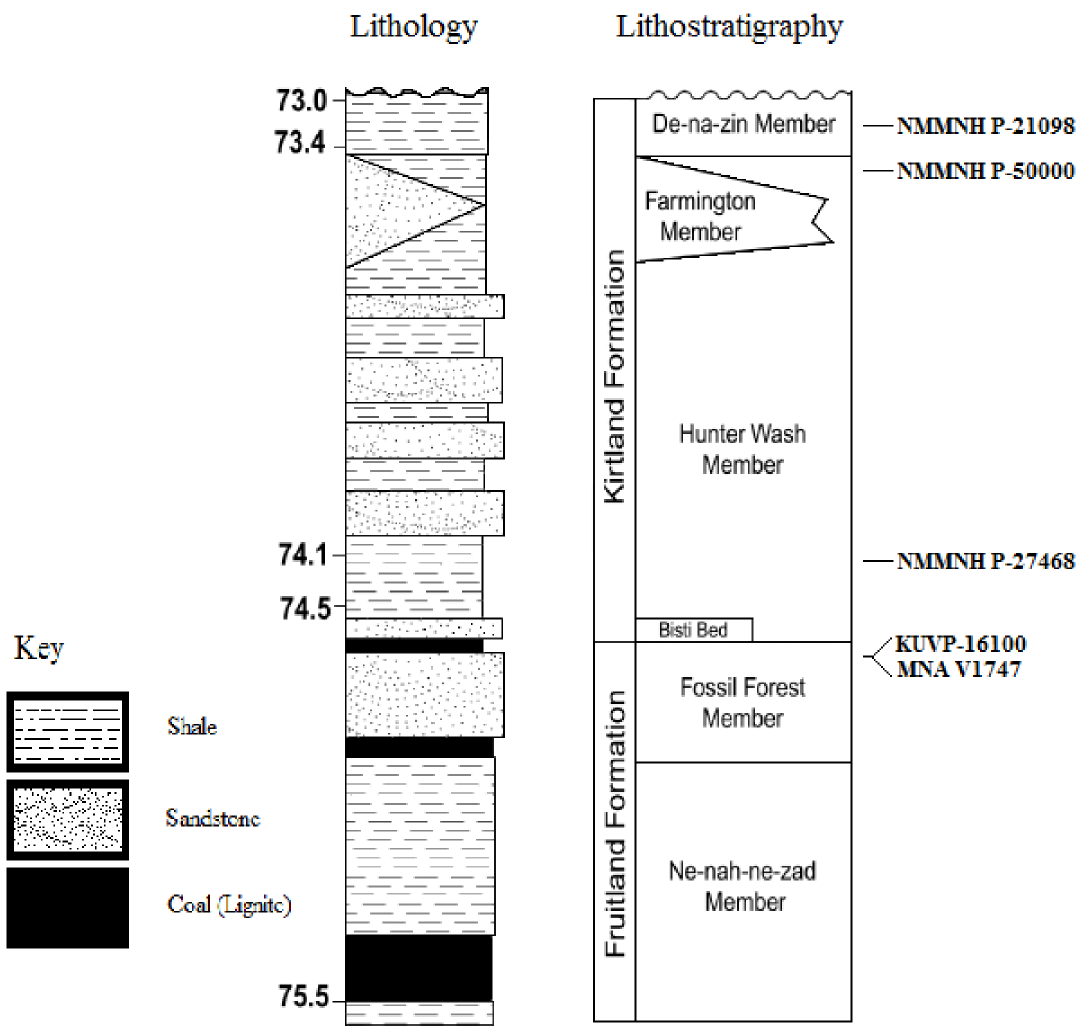

Fig. 3. Summarized stratigraphic section of the Fruitland and Kirtland formations with the stratigraphic positions of study's referred specimens. The boundary for the Fruitland and Kirtland is placed at the bottom of the "Bisti Bed". Image modified from Sullivan and Lucas (2015).

Methods

Due to the incompleteness of the original description, as it was not fully prepared, MNA V1747 is redescribed. The redescription provides insight into several cranial features that are not observed in other specimens and indicates that MNA V1747 is the most complete *Pentaceratops* skull ever found. Additionally, MNA V1747 and the four other specimens in this study were coded and photographed during visits to the Museum of Northern Arizona, University of Kansas Natural History Museum, and the New Mexico Museum of Natural History. Each specimen was individually coded by the author using the character list provided by Mallon et al. (2014) and included in two phylogenetic analyses.

Two Majority Rule Consensus tree were produced based upon the individual specimen characters collected by the author, using character states for the rest of Ceratopsia as used by Mallon et al. (2014). Mallon et al.'s (2014) character list is a modified matrix of Wick and Lehman (2013), which was previously modified from Mallon et al. (2011) and Sampson et al. (2010). The character matrix used consists of 31 taxa with 152 cranial and postcranial characters and was imported into Mesquite *v*3.02 for analysis (Appendix 1). As with previous studies (Sampson et al. 2010; Mallon et al., 2011, 2014; Wick and Lehman 2013), *Leptoceratops* is the designated outgroup for all Ceratopsia for this matrix.

Each of the five specimens varies in its respective level of completeness. The absent elements were recorded in the matrix as missing data, coded as "?". Missing data are treated as ambiguous, which mean that they are treated as a basal state (Platnick et al., 1991, Wiens, 1998). The following percentages represents the missing data in each character list out of 152 characters: (NMMNH P-21098) 86.8%, (NMMNH P-27468) 84.2%, (KUVP 16100) 63.8%, (NMMNH P-50000) 63.8%, and (MNA V 1747) 26.3%. Values were estimated using 500 replications. From these generated replicas, a majority rule consensus tree was produced and the required frequency for grouping was 0.5.

Because three specimens were used as reference material, MNA V1747, NMMNH P-27468, and NMMNH P-50000, a second consensus tree was produced excluding the *P. sternbergi* OTU. The removal of the OTU eliminated coding repetition from the tree. As a result, any difference in the recovery of the five specimens between the two trees represents actual relationships between the specimens and the other ceratopsian taxa. When evaluating the recovery of the five referred specimens of this study, taxonomic assignments are validated based upon the distance from the OTU for *P. sternbergi* in the first consensus tree and the maintaining of placement in the second consensus tree.

SYSTEMATIC PALEONTOLOGY

Dinosauria Owen, 1842

Ornithischia Seeley, 1887

Ceratopsia Marsh, 1890

Ceratopsidae Marsh, 1888

Chasmosaurinae Lambe, 1915

Pentaceratops Osborn, 1923

P. sternbergi Osborn, 1923 (formerly listed as *P. sternbergii*, emend. Lehman, 1998, p.895)

Holotype: AMNH 6325, an incomplete skull and skeleton (skeleton was discard in field) lacking the posterior portion of the parietal (except the medial bar), the right squamosal, and the posterior end of the left squamosal. Six episquamosals are present along left squamosal

Distribution: Upper Fruitland Formation (Fossil Forest Member) to lower Kirtland Formation (Hunter Wash Member), New Mexico, Williams Fork Formation, Colorado.

Etymology: *penta-* (five), *cerat-* (horn), *-ops* (face); *sternbergi* (honoring Charles H. Sternberg, the collector of the holotype)

HISTORICAL SYNONYMY

Genus *Pentaceratops* Osborn, 1923

1923 *Pentaceratops* Osborn, American Museum Novitates, 93: 1-3. Type species: *Pentaceratops sternbergii* Osborn, 1923, American Museum Novitates, 93: 1.

2010 *Titanoceratops* Longrich, Cretaceous Research 32, 264–276. Type species: *Titanoceratops ouranos* Longrich, Cretaceous Research 32: 265. (Synonymized by Sullivan and Lucas, 2015)

2015 *Pentaceratops*: Sullivan and Lucas, Sullivan and Lucas, New Mexico Museum of Natural History and Science, Bulletin 67: 287.

Pentaceratops sternbergi (Osborn), 1923

1923 *Pentaceratops sternbergii* Osborn, American Museum Novitates, 93: 1. (Emended by Lehman, 1993)

1931 *Pentaceratops fenestratus* Wiman, Nova Acta Regiae Societatis Scientiarum Upsaliensis, series 4, 7: 4. (Synonymized by Lehman, 1993)

1993 *Pentaceratops sternbergi*: Lehman, Journal of Paleontology, 9: 279.

2010 *Titanoceratops ouranos* Longrich, Cretaceous Research 32: 265. (Synonymized by Sullivan and Lucas, 2015)

2015 *Pentaceratops sternbergi*: Sullivan and Lucas, New Mexico Museum of Natural History and Science, Bulletin 67: 287.

RE-DESCRIPTION OF MNA V1747 (*Pentaceratops sternbergi)*

General Remarks

MNA V1747 is a nearly complete partially articulated skull with associated post-crania assigned to *Pentaceratops sternbergi*. The only elements missing are the lacrimals, quadratojugals, nasal horncore, supraorbital horncore bases, vomer, and the palatine bones (Fig. 4). Anterior portion of the skull displays plastic deformation. Right lateral side of nasal/premaxilla region compressed medioventrally while left lateral side stretched lateroventrally (Fig. 5). Both supraorbital horncore bases are missing, preventing reconstruction of horn orientation. Squamosal-parietal frill nearly complete with fused epiparietals and episquamosals. Postcranial elements include a nearly complete left pubis; approximately four dozen rib fragments (either cervical or thoracic) and nearly complete vertebrae (either fused or fragmented). These elements are not described in this study due to their lack of utility. All cranial measurements listed in Table 1.

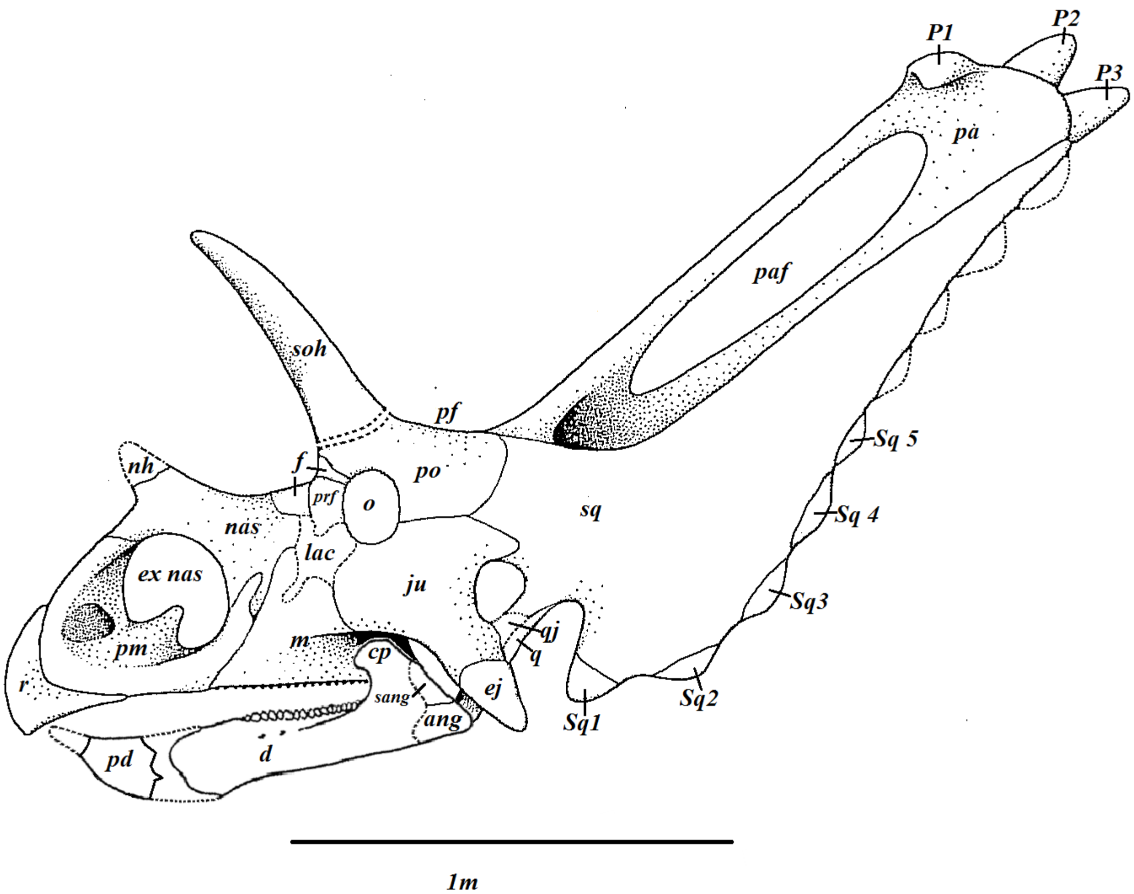

Fig. 4. Left lateral view of reconstructed skull of *P. sternbergi*. Dashed lines are elements or contacts that are absent. Illustration modified from Lehman (1993).

Table 1. Cranial Measurements of MNA V1747

Variable	Value (mm)
Rostral Bone: Length from tip to dorsal posterior flange (along curved surface)	269
Rostral Bone: Length from tip to ventral posterior flange (along curved surface)	183 L /? R
Premaxilla: Fossa maximum width	112* L /112* R
Premaxilla: Anterodorsal process dorsal surface	87 L /91 R
Premaxilla: Anterodorsal process ventral surface	51 L /81 R
Nasal: Maximum dorsal length from premax to skull roof	293* L /275* R
Nasal: Maximum ventral length from premax to skull roof	269* L /254* R
Maxilla: Maximum Length	496 L /536 R
Maxilla: Maximum Length of Occlusal Surface	403 L /348 R
Maxilla: Maximum Height	217 L /239 R
Predentary: Maximum Length	163 L /145 R
Predentary: Maximum Height	132 L /108 R
Dentary: Maximum Length	540 L /559 R
Dentary: Maximum Length of Occlusal Surface	368 L /381 R
Dentary: Maximum Height to Occlusal Surface	176 L /174 R
Dentary: Maximum Height to Coronoid Process	215 L /227* R
Surangular: Maximum Length	128* L /132 R
Surangular: Maximum Width	61 L /62 R
Fused Articular/Angular: Maximum Length (Anterior-Posterior)	153 L /175 R
Fused Articular/Angular: Maximum Width (Medial- Lateral)	178 L /143 R
Fused Articular/Angular: Maximum Wdith of Quadrate Groove	73 L /66* R
Jugal: Maximum Length (Dorsal-Ventral)	276 L /426 R
Jugal: Maximum Width (Anterior-Posterior)	197 L /304 R
Epijugal: Maximum Length (Dorsal-Ventral)	82 L /81 R
Epijugal: Maximum Width (Anterior-Posterior)	60 L /86 R
Quadrate: Maximum Length (Dorsal-Ventral)	218 L /354* R
Quadrate: Maximum Width of Lateral Edge to eminence of the Pterygoid (Medial-Lateral)	99 L /? R
Quadrate: Maximum Width of Articular Process (Medial-Lateral)	72 L /116 R
Quadrate: Maximum Width of Squamosal Process (Medial-Lateral)	? L /157* R
Pterygoid: Maximum Length (Anterior-Posterior)	332 L /178* R
Pterygoid: Maximum Height (Dorsal-Ventral)	163 L /151* R
Occipital Condyle: Circumference	225
Occipital Condyle: Diameter (Use of Helios dial Caliper accurate to 1/20 a mm)	71.9
Excoccipitals: Maximum distance from Occipital Condyle	244 L /175 R
Maximum Width between Basioccipital Tubers	202
Maximum Width between Basipterygoid Processes	156
Supraorbital Horncores: Maximum Length (tip to base, straight line)	553* L /641 R
Supraorbital Horncores: Maximum Girth	442 L /446 R (as preserved)
Fused Prefrontals/Frontals	? L /? R
Crushed Postfrontals	? L /? R
Squamosal: Maximum Length (Sq1 to the distal tip of the blade)	1272 L /1273 R
Squamosal: Maximum Width (Anterior portion that articulates to skull roof)	401 L /542 R
Squamosal: Minimum Width (Posterior end of blade)	17 L /19 R
Parietal: Maximum Width (Anterior)	528
Parietal: Maximum Width (Posterior)	258
Parietal: Maxium Width of U shaped opening (Straight line, middle of P2 to P2)	158
Parietal: Medial Bar Length (Broken anterior contact to bottom of U shaped opening)	655
Parietal: Medial Bar Maximum diameter	216 A /196 P
Parietal: Medial Bar Minimum diameter	134

Note: Bilateral measurements are given as left (L), right (R), anterior (A) and posterior (P). Measurements marked with an asterisk (*) have been estimated.

Rostral Bone

Rostral relatively complete; slight distortion on left lateral side and significant distorted on right lateral side (Fig. 5). Shape of rostral pyramidal, angled posteriorly. Rostral forms tip anteroventrally, recurves posterodorsally. Two processes expand laterally from anteroventral tip to form ventral surface. Surface on ventral edge of lateral sides rugose. Dorsal surface of lateral faces of rostral fractured, but surface relatively smooth. Ventrolateral processes slightly concave. Left ventrolateral process present, but contact between ventrolateral process and right premaxilla cannot be distinguished due to distortion (Table 1). Dorsolateral edge of right side missing section of bone that would rest under premaxilla (Fig. 5). Both posteroventral processes and posterodorsal process envelope premaxilla.

Premaxilla

Premaxilla present with slight lateroventrally expanded left lateral side; right lateral side severely deformed and medially compressed. Premaxilla compressed medially forming shallow premaxillary fossa anterior to rostral bone (Fig. 5). Bone of premaxillary fossa very thin. Interseptal foramen perforates premaxillary fossa. Due to fragile nature of premaxillary fossa and sharp broken edges, interseptal foramen appears to be result of fragmentation.. Small single triangular process intrudes into foramen. Premaxillary fossa relatively circular in shape, but deformation prevents accurate measurement (Table 1). Premaxillary fossa partially overlapped posteriorly by robust nasal strut (Fig. 5). Nasal struts bifid, angled posteriorly, and separated by medial indentation on posterior side. Both right and left processes are present. Premaxillary process posteroventral to each nasal strut. Process triangular and extrudes into anterior wall of external naris.

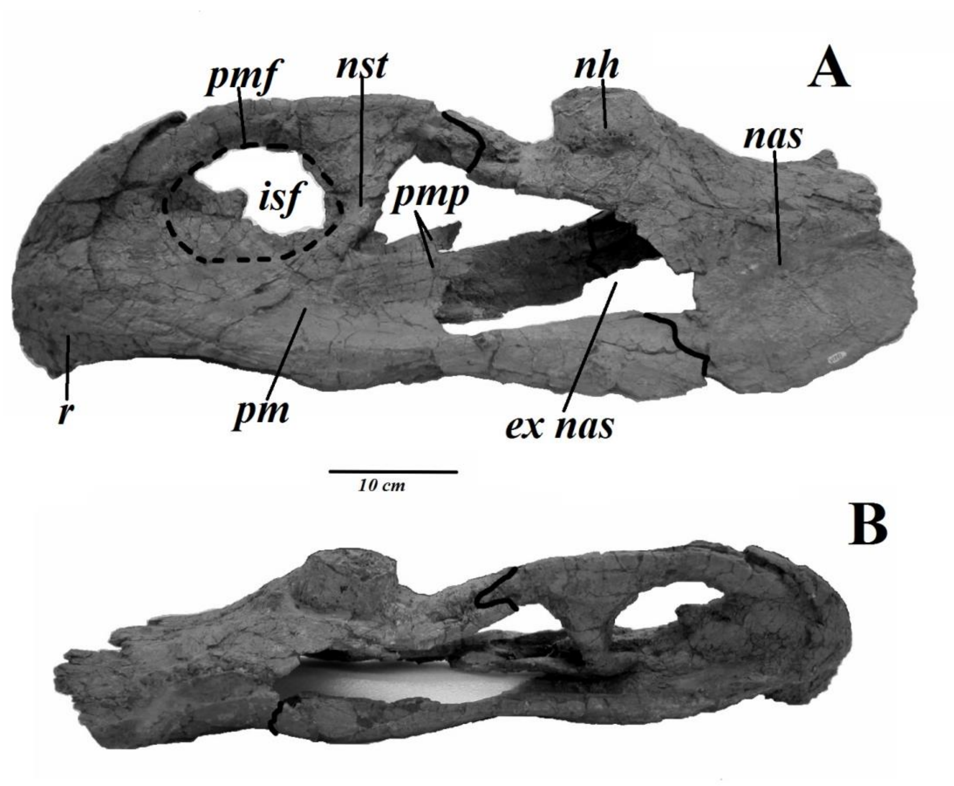

Fig. 5. Articulated rostral bone, premaxillae, and nasals of MNA V1747. (A) Left lateral view and (B) Right lateral view. Abbreviations: Dashed lines outline premaxilla fossa. Suture contacts between premaxillae and nasal marked in black. (Photos by J.J. Fry courtesy of the Museum of Northern Arizona)

Prominent depression along dorsal margin of premaxilla divides premaxilla into left and right lateral faces. Posterodorsal-most margin of depression curves ventrally under anterodorsal nasal bone. Ventral indentation of premaxillae forms part of dorsal roof of external naris with dorsal suture contact visible (Fig. 5). At articulation with nasals, straight suture forms transverse surface just anterior of nasal horncore. Suture continues on ventral side of dorsal margin of external naris forming relatively straight margin. Posteroventrally, premaxilla thins forming posteroventral processes of premaxilla, which articulates with nasal bone dorsally to form ventral base of external naris and dorsal contact of maxillae. Due to distortion, contacts with maxillae not preserved.

Nasal

Nasals present and elongated (Fig. 5). Dorsal contact with premaxilla forms straight suture that intersects dorsoposterior surface of premaxilla just anterior to nasal horncore. Ventral contacts ventral to posteroventral processes of premaxilla. Length of nasals forms contact with premaxilla to skull roof varies depending on side of skull (Table 1). Articulations with maxilla on both left and right lateral sides not preserved. Posterior margin of nasals broken and distorted. Articulation contacts with frontals and prefrontals not preserved. Nasals relatively smooth with exception of nasal horncore base.

Left lateral side of nasals appears only slightly distorted due to medial expansion. Posterior margin of left external naris rounded triangular in shape, dorsal margin remains fairly close to mid line of snout (Fig. 5). As left nasal continues posteriorly, ventral edges expand outward laterally to form ventroposterior margin of external naris. Distortion due to dorsal-ventral compression has crushed right lateral side and ventral margin of nasal has moved medially. Right external naris extremely distorted and shaped like stretched out ellipse. Nasal horncore sits on mid line of snout directly above posterior half of external naris (Fig. 6). Only base of nasal horncore preserved. In cross section, shaped like reuleaux triangle and oriented anteriorly. Ventral base texture of horncore contains evidence of vascular grooves and internal texture of broken dorsal edge has spongy texture.

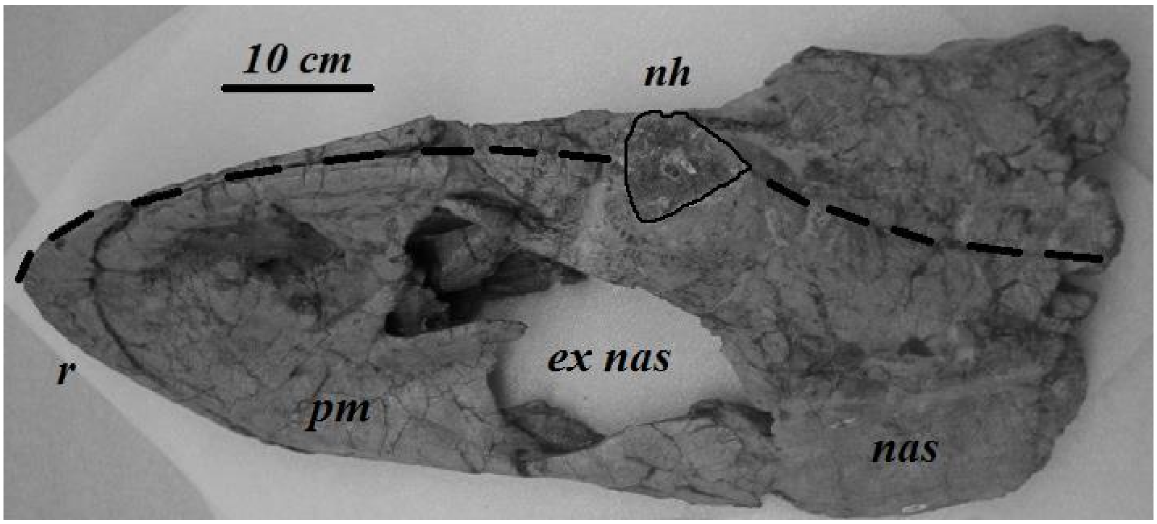

Fig. 6. MNA V1747 in dorsal view showing rostral/premaxillae/nasal elements. Nasal horn outline in black. Dashed line indicates midline of skull. (Photo by J.J. Fry courtesy of the Museum of Northern Arizona)

Maxilla

Both right and left maxillae present and disarticulated from rest of skull (Fig. 7). Maxillae have triangular shape with anterior potion forming point. Expanding posteriorly, dorsal margin extend posterodorsally while ventral margin remain relatively straight. Teeth angled slightly medially in both maxillae. Occlusal surface forms nearly horizontal plain. Posterior end forms circular indentation separating into two tampering processes. Right maxilla medial side exhibits series of foramina for nutrient canals leadings to tooth row; absent from left maxilla. Medial surface of both maxillae exhibits large semicircular pterygoid groove. This pterygoid groove, in combination with tampered posteroventral margin, houses palatine, vomer, and pterygoid. Laterally, indentation of maxillae forms anterior and ventral margins of opening between maxillae and jugals where coronoid process articulates.

Right maxilla more fractured with plaster filling in missing fragments (Fig. 7 A-B). More of anteroventral bone and posterodorsal bone present than on left maxilla. Posteroventral process more robust than left maxilla. Five foramina observed on lateral surface dorsal to tooth row (compared to the two on left). Teeth present, but tooth row slightly pushed into right maxilla, less exposed than on left. Within right tooth row, 18 teeth present with empty sockets. Unlike left maxilla, teeth preserved in right maxilla evenly dispersed throughout tooth row. Length of right maxilla tooth row accounts for 64% of total right maxilla length (Table 1).

Left maxilla undistorted, but may be missing bone from its posterodorsal region where articulation with jugal and lacrimal would occur (Fig. 7, C-D). Two foramina dorsolateral to tooth row of left maxilla. Twenty-three teeth present in different stages of development. Anterior teeth missing and only empty sockets remain. Maximum length of left maxilla tooth row accounts for 81% of total left maxilla length (Table 1).

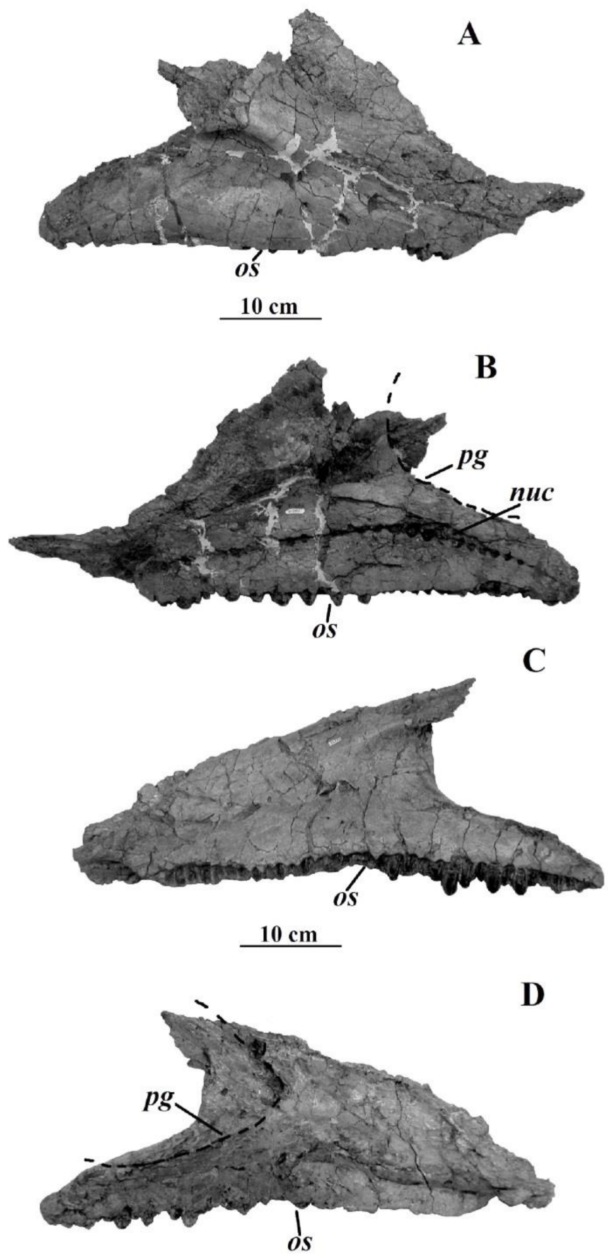

Fig. 7. Maxillae of MNA V1747. (A, B) Right maxilla lateral view and medial view (C, D) left maxilla lateral view and medial view. Dashed line indicates surface of pterygoid groove. (Photos by J.J. Fry courtesy of the Museum of Northern Arizona)

Predentary

Predentary present, but partially incomplete and contains large amount of plaster holding it together (Fig.8). Shaped as dorsally curved triangular pyramid. Dorsal edges concave anteriorly and become horizontal in respect to dentary. Ventral edge curved anteriorly and becomes horizontal along dorsal edges posteriorly. Ventral edge formed by contact of right and left lateral surfaces of predentary. Right lateral surface slightly compressed medially and left lateral surface slightly expanded laterally. Left lateral surface more complete than right (Table 1). Anterior end of predentary with vascular grooves on its lateral surface and few to no vascular grooves on medial surface. Posterior end with fewer vascular grooves. Anterior tip of predentary and most of posterior contact with dentaries not preserved. Dorsal surface of predentary depressed where rostral and premaxilla would rest, while anterodorsal margin absent from right side.

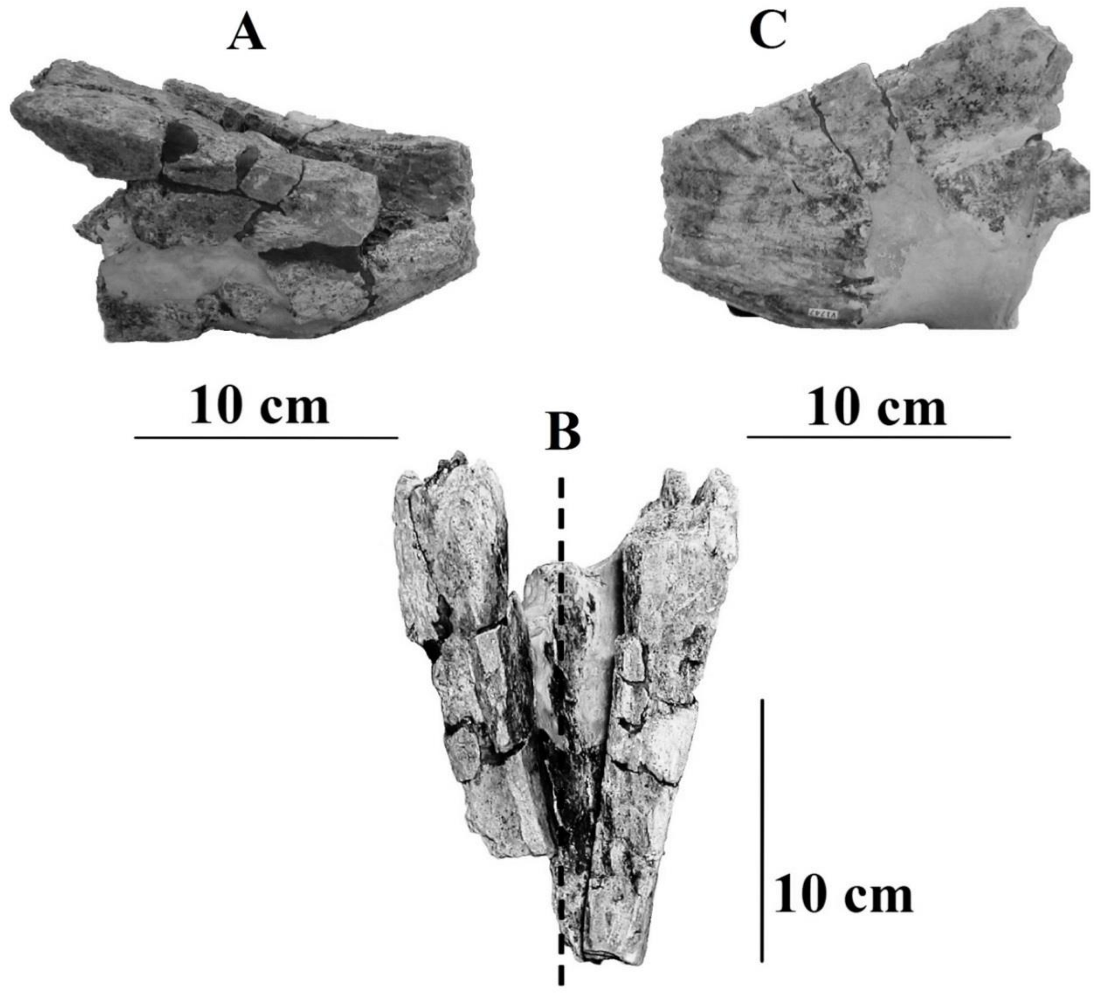

Fig. 8. Predentary of MNA V1747, (A) right lateral view, (B) dorsal view, and (C) left lateral view. Dashed line indicates midline of skull. (Photos by J.J. Fry courtesy of the Museum of Northern Arizona)

Dentary

Pair of disarticulated and nearly complete dentaries present (Fig. 9). Dentaries oblong in shape with coronoid process rising almost perpendicular to ventral surface. Anterior ends compressed medial-laterally to form blade. Anterodorsal margin of blade angled laterally while anteroventral margin angled medially in respect to tooth row. Blade's anterior most surface forms a grooved symphysis and contacts for predentary. Dentaries thicker posteriorly as tooth row forms on dorsal margin. No lateral ridge ventral to coronoid process present on lateral surface of dentaries. Mandibular fossa present along ventromedial surface of both dentaries (Fig. 9). In both dentaries, all teeth present in tooth row angle laterally slightly. Occlusal surface of tooth row forms nearly horizontal surface to occlude with maxillary teeth. As tooth rows continue posteriorly, process on lateral edge of dentaries forms anteroventral base of coronoid process. Space between tooth row and coronoid process housed jaw muscles. Nearly complete coronoid process for both right and left present. Contacts with angular and subangular not preserved.

Right dentary similar to left (Fig. 9 A-B), but anterodorsal edge of left coronoid process and ridge absent. Surface details not well preserved on right dentary and ventral margin reconstructed with plaster. Three lateral foramina, ventral to tooth row, present. Right dentary contains 24 teeth and no empty sockets present. Posterior end of tooth row and small process that connects tooth row to coronoid missing. Right occlusal surface length accounts for 68% of total length of right dentary (Table 1).

Left dentary (Fig. 9 C-D) more complete then right. Left coronoid process with subangular to rounded edges and anteriorly angled at its dorsal margin. Left coronoid process fractured at base and compressed slightly medially to form a ridge. Six foramina visible and ventral to tooth row on lateral side. Left dentary contains 27 teeth of various sizes and stages of growth, as well as empty sockets. Left occlusal surface length accounts for roughly 68% total length of left dentary (Table 1).

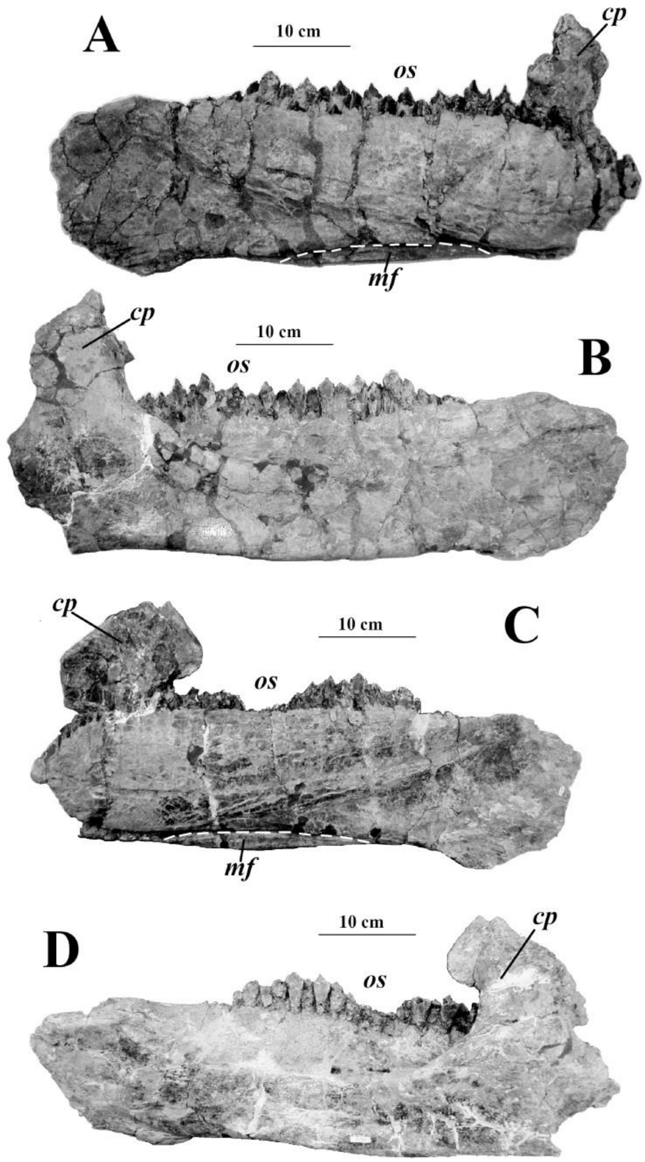

Fig. 9. Dentaries of MNA V1747, (A, B) right dentary medial view and lateral view (C, D) left dentary medial view and lateral view. Dash line marks mandibular fossa. (Photos by J.J. Fry courtesy of the Museum of Northern Arizona)

Articular/Angular

Both articulars and angulars present and fused to one another. Articulars roughly rectangular in shape with round groove where quadrate contacts. Left articular better preserved and has more complete quadrate groove. Unlike right articular, left articular does not display dorsal arching of ventral surface. Dorsal process on left angular broken and compressed medially. Anterior margin of left angular/articular complex loosely fits to ventroposterior groove of left dentary. Right angular fragmented and contains dorsally expanding process. Process fragmented and reconstructed. Anterior margin of right angular/articular complex lacks full articulation to right dentary's ventroposterior groove of due to fragmentation.

Surangular

Both surangulars fairly complete, dorsoposteriorly angled process broken on both left and right surangulars (Fig. 10 A-B). Left surangular broken into two pieces held together by plaster, with no significant influence on its dimensions (Table 1). Neither surangular appears to have any articulation surfaces to angulars due to distorted natural of those elements, but both loosely fit within dorsoposterior groove of dentaries.

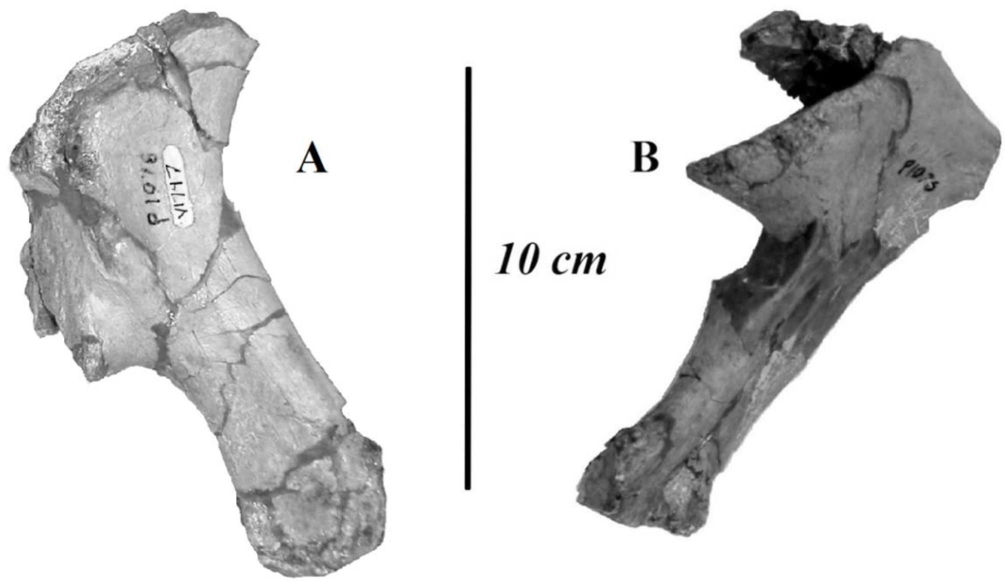

Fig. 10. Surangulars of MNA V1747. Right surangular (A) medial view and Left surangular (B) medial view. (Photos by J.J. Fry courtesy of the Museum of Northern Arizona)

Jugal

Both jugals present but fragmented and distorted (Fig. 11). Both triangular in shape with apex forming point ventrally and base dorsally. Dorsal margin forms ventral wall of orbit. Jugal articulates anteriorly with missing lacrimal, posterodorsally with postfrontal, posteriorly with squamosal, posteroventrally with missing quadratojugal, and ventrally with epijugal. Due to disarticulation and distortion, epijugal articulation surfaces not preserved. Left jugal poorly preserved and incomplete (Table 1). Left jugal does not articulate to rest of skull and ventral margin of left orbit not preserved. Most of orbital margin intact on right jugal. Articulations to other skull elements for right side lost or distorted. Dorsal side of jugals rugose and vascular grooves prominent on right jugal. Ventrally, bone smooth with visible fractures.

Epijugal

Both epijugals present, unfused and disarticulated to jugals, robust and trihedral in shape (Fig. 11). Epijugals curve posteriorly and rugose with longitudinal vascular grooves at base. Left and right roughly same length, but vary in width (Table 1).

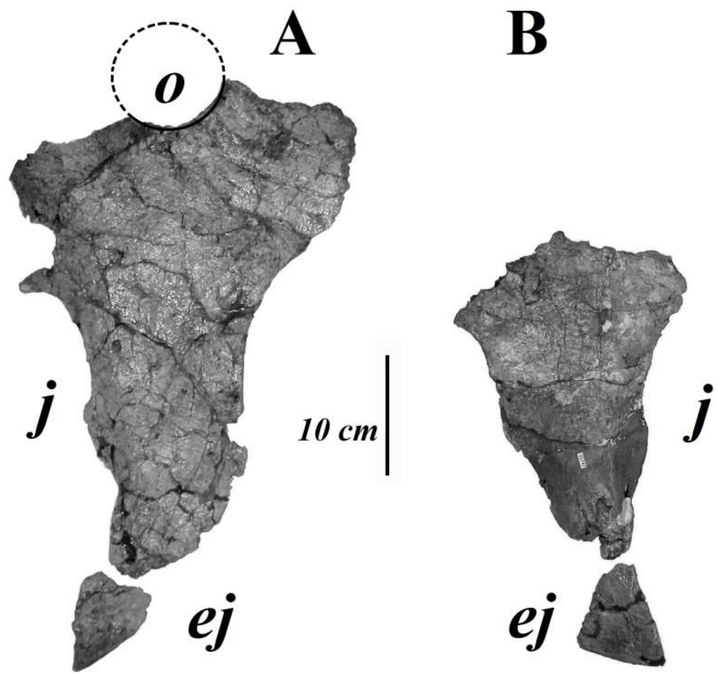

Fig. 11. Jugals with associated epijugals of MNA V1747 in lateral view. Right Jugal (A) left Jugal (B). Dash line indicates missing margins of orbit. (Photos by J.J. Fry courtesy of the Museum of Northern Arizona)

Quadrates

Right quadrate compressed anterior-posteriorly resulting in mediolateral expansion (Fig. 12, A-B). Pterygoid process and eminence absent from right quadrate and largely reconstructed with plaster. Dorsal margin forms squamosal process while ventral margin forms articular process. Right squamosal process contains substantial amount of plaster reconstruction and tapers to thin strip due to mediolateral expansion.

Left quadrate less distorted (Fig. 12, C-D). Squamosal process of dorsal margin absent, but articular process present. Absence of squamosal process on left accounts for difference in dimensions between quadrates (Table 1). Along lateral midline, small process of bone present that represents ventral margin of pterygoid eminence. On posterior face, lateral surface of left quadrate folds medially forming large groove, which forms articulation surface for pterygoid.

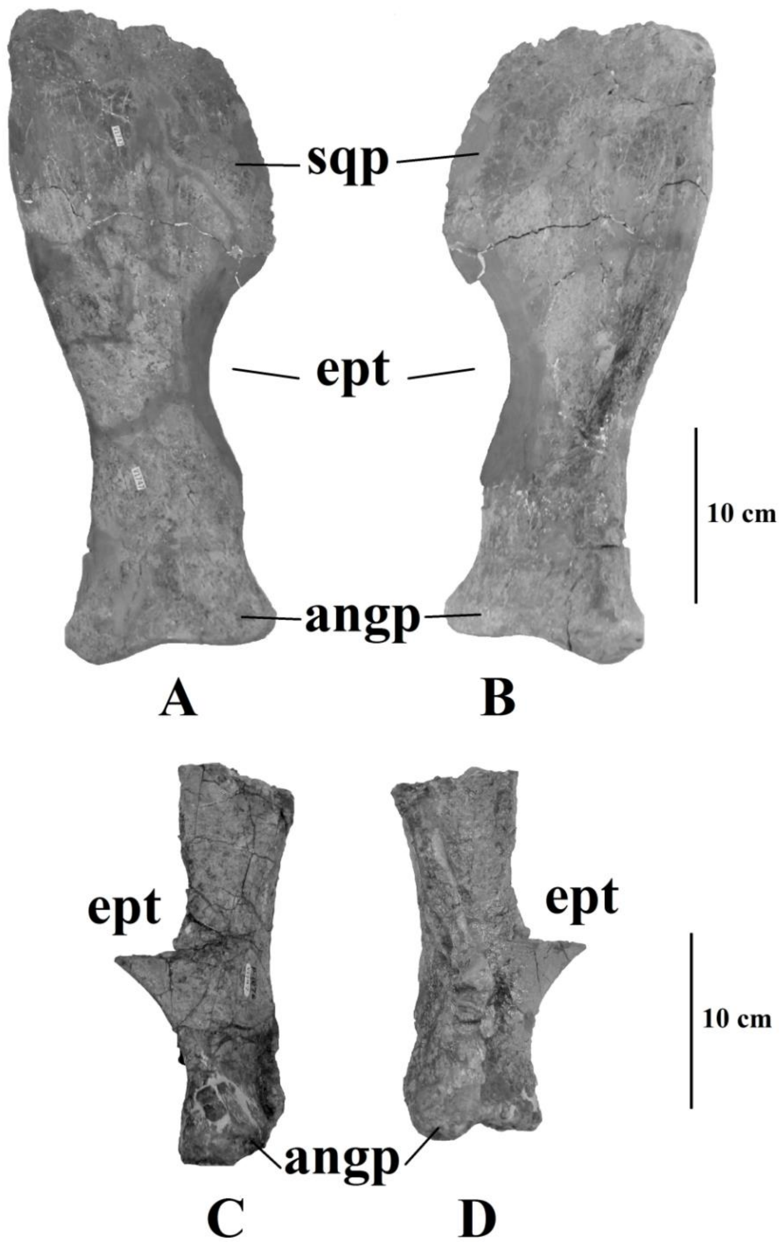

Fig. 12. Quadrates of MNA V1747. Right quadrate (A-B) anterior and posterior views left quadrate (C-D) anterior and posterior views. (Photos by J.J.Fry courtesy of the Museum of Northern Arizona)

Pterygoids

Both pterygoids present (Fig. 13). Right pterygoid more damaged than left with both elements exhibiting mediolateral compression, distorting true dimensions of elements (Table 1). Lateral curvature on right pterygoid shortens element's maximum height. Majority of anterior portion of right pterygoid lost, particularly process forming palatine groove. Left pterygoid nearly complete.

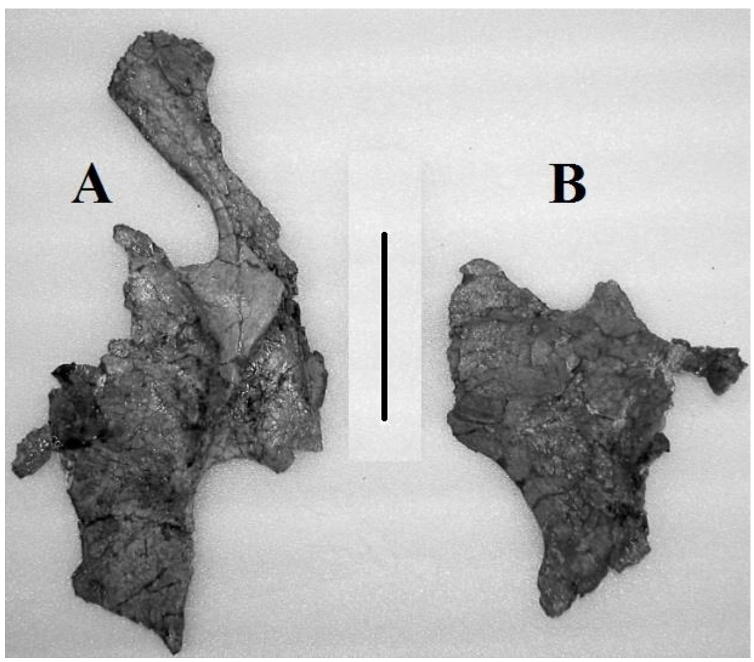

Fig. 13. Lateral view of left (A) and right (B) pterygoids of MNA V1747. Top of image anterior, bottom posterior. Scale bar represents 10 cm. (Photo by J.J. Fry courtesy of the Museum of Northern Arizona)

Braincase

Braincase nearly complete but slightly dorsoventrally compressed. Braincase and overlying skull bones form largest structure of skull. Although compressed, symmetry of braincase offset by less than 20 mm to left from midline (Fig. 14). Dorsoventral compression and slight lateral movement occurred after burial. Supraoccipital fused to dermatocranial elements. Due to fusion, internal structures such as inner ear or endocranial cavity cannot be observed.

Basipterygoid processes preserved, but anterior articulation to pterygoids not preserved. Right basipterygoid shifted medial due to compression. Posterior to basipterygoids, basioccipital forms central element of braincase. Basioccipital rugose with several large vascular canals etched onto ventral surface. Texture diminishes laterally in all directions from basioccipital on any of articulating processes. Posterolateral to basipterygoids and lateral to basioccipital; fused basioccipital tubers robust and bulbous. Exoccipitals expand posterolaterally from basioccipital. Right exoccipital incomplete and smaller than almost complete left exoccipital. Complete and undistorted occipital condyle fused posterior to basioccipital. Foramen magnum dorsal to occipital condyle. Foramen magnum elliptic due to compression; cranial nerve foramina that surround occipital condyle and foramen magnum not preserved. Paroccipitals and paroccipital processes posterior to occipital condyle not preserved.

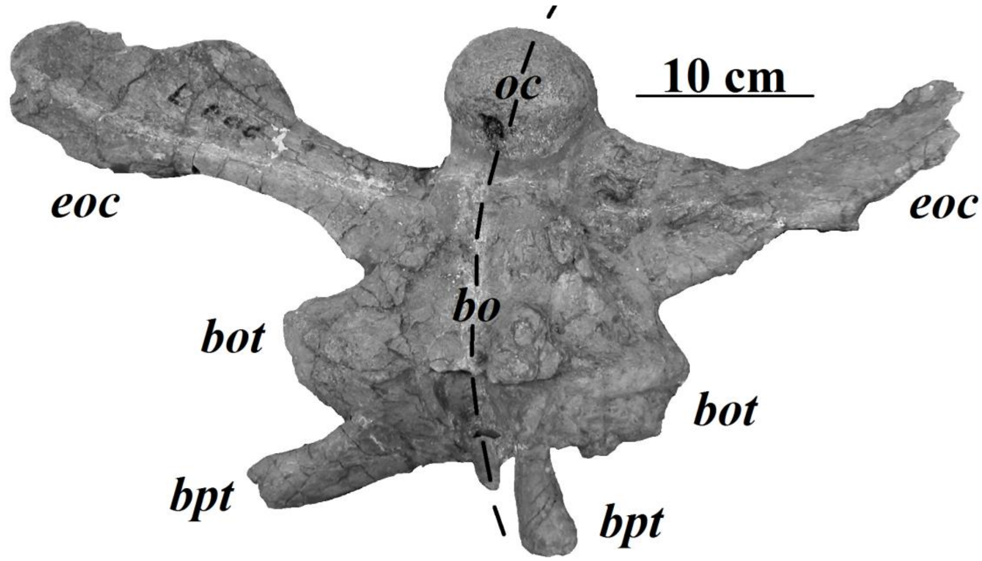

Fig. 14. Ventral view of braincase of MNA V1747, (Foramen magnum and supraoccipital are not visible in ventral view). Dashed line indicates approximate original midline of skull preceding taphonomic distortion. (Photos by J.J. Fry courtesy of the Museum of Northern Arizona)

Postorbital

Both postorbitals present, but area of articulation to supraorbital horncores not preserved (Fig. 15). Sutures between frontals and postfrontals indistinguishable dorsally and ventrally due to co-ossification of skull roof. Postorbital form dorsal margin of orbit. Right postorbital only slightly distorted while left supraorbital dorsolaterally distorted and distorts left orbit.

Supraorbital Horncores

Both supraorbital horncores broken off from rest of skull and broken pieces no longer articulate. Both horncores angle anteriorly and curvature cannot be identified due to lack of articulation surface with postorbitals. Based on shape of horncore base and broken edge, it is possible to determine left from right. Right horncore longer and mediolaterally compressed. Left horncore less distorted, circular, and with broken base. Left horncore lacks distortion, smaller than right, with incomplete anterior tip (Table 1). Horncores rugose at bases with longitudinal vascular grooves.

Prefrontal

Both prefrontals preserved, but articulation sutures obscured due to co-ossification with postorbitals and frontals (Fig. 15). Prefrontals form anterodorsal margin of orbit and anteriorly articulate to lacrimals. Lacrimals and articulation surface to prefrontals not preserved. Large growth of bone present on left prefrontal. Sharp edged nature of bone texture likely due to taphonomic process exerted on prefrontal rather than pathology (Fig. 15 A). Right prefrontal less distinct and lacks bony growth observed on left (Fig 15 B).

Frontal/Postfrontal

Frontals and postfrontals indistinguishable from each other and adjacent elements (Fig. 15). Frontals bordered anteriorly by nasal and posteriorly by postfrontals; prefrontals articulate anterolaterally to frontals. Postorbitals articulate anterolaterally to frontals. Frontals play minor role in formation of orbits. Postfrontals bounded anteriorly by frontals, anterolaterally by postorbitals, posterolaterally by squamosals and posteriorly by parietal. Postfrontals form posterior wall of orbits. Postfrontal fontanelles on posterior margin of postfrontals. Structures elongated semicircular depressions that close anteriorly and open posteriorly. Left lateral side of postfrontal fontanelles margin reconstructed with plaster. Right lateral side contains two openings that lead to right orbit. Openings have sharp edges and occur in thinnest part implying possible diagenetic origins. Frontals and postfrontals rugose with shallow vascular grooves.

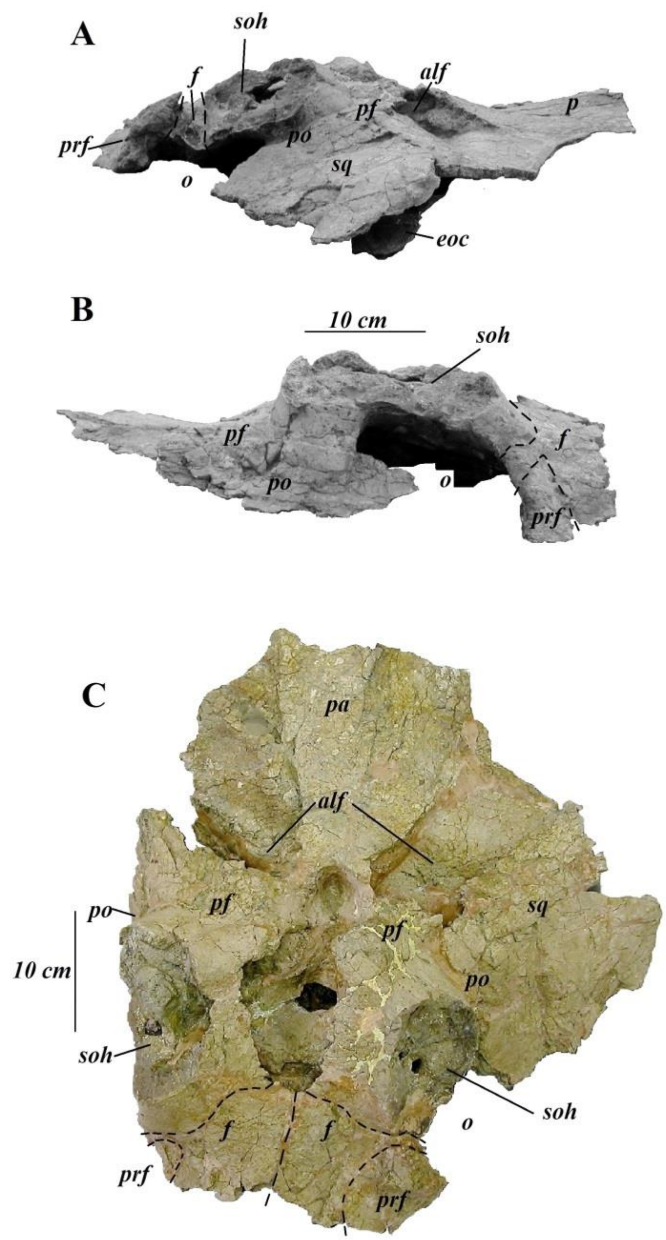

Fig. 15. Skull roof of MNA V147. (A) Left lateral view, (B) right lateral view, and (C) dorsal view of skull roof elements. Dash lines mark visible sutures of the frontals with adjacent elements. (Photos by J.J. Fry courtesy of the Museum of Northern Arizona)

Squamosals

Both squamosals present with similar proportions (Table 1). Anterior part of each squamosal missing fragments or fractured. Both squamosals wide and robust anteriorly and tamper to rounded point posteriorly. Lateral margins shift slightly medially from anterior to posterior.

Proximally, right squamosal broken into two separate elements and appears to preserve natural curve (Fig. 16). Anterior most part articulates to skull roof just posterior to supraorbital horns. This piece of right squamosal continues posteriorly largely intact. Smaller element separated by simple mediolateral break from larger anterior portion in upper forth of right squamosal. Only posteromedial part of right squamosal articulates to parietal. Contact forms overlapping groove allowing lateral margin of parietal to interlock with right squamosal. Bone that lies between medial and lateral margins of right squamosal depressed forming convex surface. Dorsal side of right squamosals rugose and covered with vascular grooves. Anterior grooves radiate from medial part of squamosal and become longitudinal towards posterior end. Texture of ventral side has subtle vascular grooves and only faint traces of vascular grooves can be identified on lateral edge.

Left squamosal broken into four parts and compressed anterior-posteriorly compared to right squamosal (Fig. 16). Left squamosal broken just anterior of first episquamosal. Small piece of left squamosal remains fused to skull roof just posterior of supraorbital horns. Left squamosal breaks into second fragment just above right jugal notch. Rest of left squamosal broken into three articulating pieces. Left squamosal tapers to point posteriorly. Left lateral margin curves medially as medial margin expands laterally. Contact with parietal nearly complete on left medial squamosal margin. Differing from right squamosal, area of bone between medial margin and lateral margin forms concave surface on anterior side and convex surface on posterior side. Texture of left squamosal same as right.

Episquamosals

Four distinguishable episquamosals on lateral margin of each squamosal observed. One additional episquamosal missing from left squamosal when compared to positions and spacing of episquamosals on right squamosal. Nine additional disarticulated episquamosals cataloged with specimen, but lack of articulation surfaces on posterior lateral edge of squamosals prevent placement of these elements. With inclusion of disarticulated elements each squamosal would have at least nine episquamosals. First episquamosal forms posterior wall of jugal notch and has a rounded triangle shape on both sides. Posteriorly, episquamosals become semicircular in shape, longer (proximal-distal) than wide (medial-lateral). Left episquamosals better preserved than those on right. Episquamosals rugose while covered in longitudinal vascular grooves.

Parietal

Parietal largely intact; only part of anterolateral wall of right parietal fenestra not preserved. Slight distortion formed small gaps along anterior margin of parietal at contact with rest of skull roof and left squamosal. Medial bar of partial complete and bears vascular grooves on its dorsal surface. Diameter of middle section of medial bar significantly less than anterior and posterior ends (Table 1) forming stretched hour glass shape. Dorsal side of medial bar slightly concave while ventral side slightly convex. Combination of concave/convex surfaces gives medial bar slight raised ridge on its dorsal side. Keyhole feature at posteromedial end of parietal forms wide "U" shape (Fig. 16).

Parietal fractured anteriorly just past anterolateral temporal fossa (Fig. 17). Anterior parts of parietal still attached to medial bar and form anterior walls of parietal fenestrae. Left parietal fenestra elongated asymmetric ovoid shape except for posterior edge angled as it expands outwards laterally. Right parietal fenestra partially complete. Anterolateral wall of right parietal not preserved, but posterior end of this wall present. Both right and left lateral margins interlock with squamosals.

Epiparietals

Three epiparietals pairs laterally expanded from each side of parietal medial bar (Fig. 18). All three epiparietals contacts co-ossified. First epiparietals (P1) articulate with parietal surface, robust at base, and taper dorsally. Paired P1s angled anterolaterally, curving posteriorly towards dorsal edge. Each P1 arched in shape with anterior curve longer than its posterior curve. Moving laterally along, paired second epiparietals (P2) form part of posterior limit of keyhole. P2s curve medially. Lateral to P2s and medial to squamosal/parietal contact third epiparietals pair (P3). P3s form posterior edge of parietal's posterolateral margin with very rounded shape. . All of epiparietals rugose and have vascular grooves that run ventral-dorsal from parietal contacts.

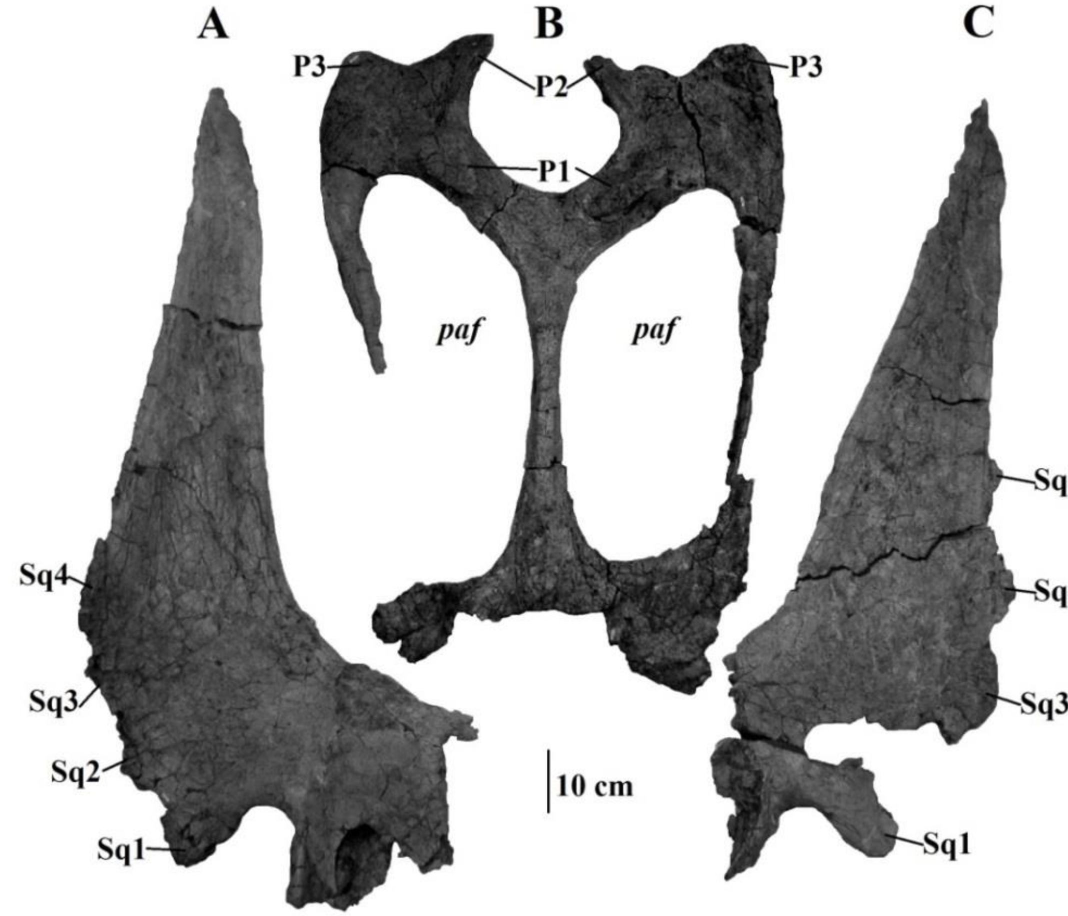

Fig. 16. Anterior view of squamosal-parietal complex of MNA V1747. Right (A) and left (C) squamosals are present and nearly complete with parietal (B). (Photos by J.J. Fry courtesy of the Museum of Northern Arizona)

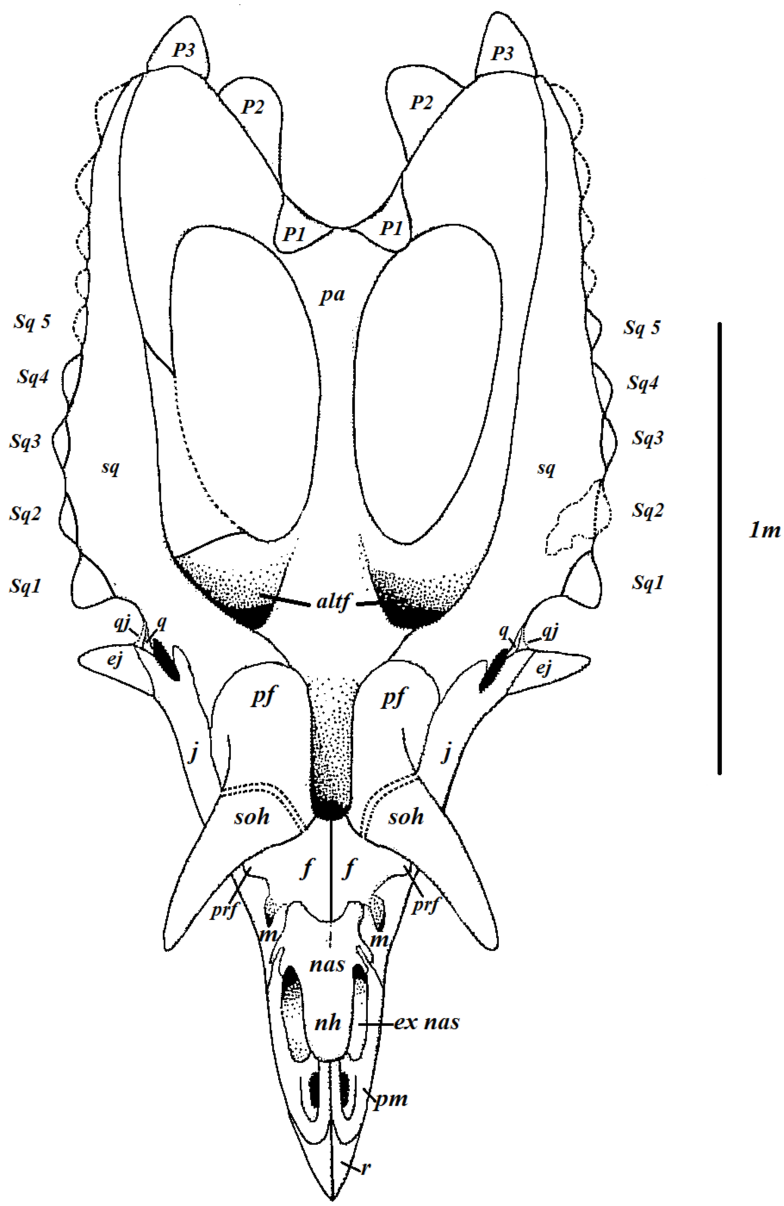

Fig. 17. Dorsal view of reconstructed skull of *P. sternbergi*. Dashed lines are elements or contacts that are absent. Illustration modified from Lehman (1993).

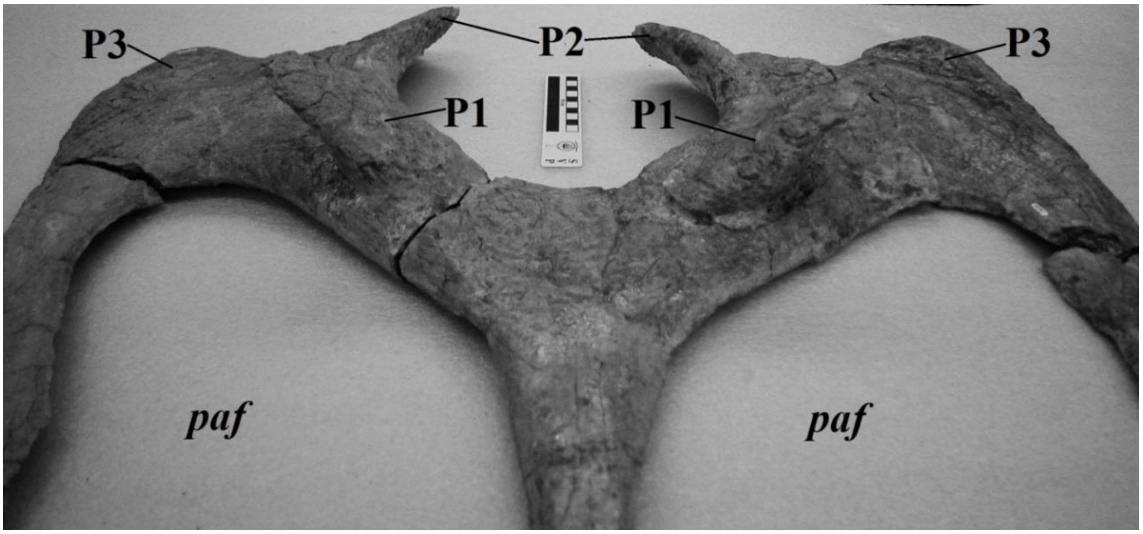

Fig. 18. Oblique view of posterior parietal U-shaped keyhole. Scale bar is 10 cm. (Photo by J.J. Fry courtesy of the Museum of Northern Arizona)

CLADISTIC ANALYSIS

The redescription for MNA V1747 reveals cranial features that differ from the four other coded specimens, as well as the OTU. These features include differing elements that form the orbit and the absence of a structure on the dentaries. All other characters observed in MNA V1747 as well as the other four specimens included in the OTU in previous studies displayed a majority of similar character states as recorded in the OTU

The first resulting majority rule consensus tree has a tree length (TL) of 311 steps, a consistency index (CI) of 0.63, and retention index (RI) of 0.754 (Fig. 19). These values are similar to results reported in most Mallon et al.'s (2014) study, TL of 338 steps, CI of 0.527, and RI of 0.634 (Sampson et al. 2010; Mallon et al., 2011, 2014; Wick and Lehman 2013) (Fig. 2). MNA V1747, NMMNH P-50000, and KUVP-16100 are recovered with the OTU forming a sister clade to *Utahceratops gettyi* (Fig. 19). The topology reveals KUVP-16100 as the sister group to a polytomy consisting of the *Pentaceratops* OTU, MNA V1747, NMMNH P-50000, grouped with *Bravoceratops polyphemus* (Fig. 19). NMMNH P-50000, MNA V1747, and the OTU grouping had a frequency of 51.2%. NMMNH P-27468 and NMMNH P-21098 are recovered outside the *Pentaceratops* clade. NMMNH P-27468 is recovered closer to the *Chasmosaurus* clade than to *Pentaceratops*. Specimen NMMNH P-21098 is recovered outside of chasmosaurine clade and is instead recovered among centrosaurines.

A second phylogenetic analysis was performed eliminating the *Pentaceratops* OTU (Fig.20). This tree has values that are similar to the first consensus tree: TL of 315 steps, CI of 0.622, and RI of 0.736. In the second majority census tree, MNA V1747, NMMNH P-50000, and KUVP-16100 form a clade in the same position as the tree with the OTU. However, *U. gettyi* and *B. polyphemus* are both found within the *Pentaceratops* clade (Fig. 20). NMMNH P-21098 is found within a polytomy that includes *Ojoceratops fowleri*, *Eotriceratops xerinsularis*, and *Arrhinoceratops brachyops*. NMMNH P-27468 ends up closer to the genus *Chasmosaurus* than to the genus *Pentaceratops*.

DISCUSSION

The redescription of MNA V1747 includes features and elements such as the absence of the lateral ridge ventral to the coronoid process and the presence of the frontals in the formation of the orbits. These are not seen in any other *Pentaceratops* specimens and should be added to the OTU since MNA V 1747 is the most complete reference specimen. Additional elements, most notably the parietal keyhole and epiparietals, have been reconstructed on the holotype based upon MNA V1747. Based on the completeness of MNA V1747 and the difficulty accessing AMNH 6325, the redescription of MNA V1747 should serve as the standard for defining *P. sternbergi* until the holotype is thoroughly coded and redescribed.

The recovery of MNA V1747, NMMNH P-50000, and KUVP-16100 within the OTU clades (Fig. 18) supports Rowe et al.'s (1981) original assignment of these three specimens to *P. sternbergi*. The polytomy grouping in the first tree between the OTU, MNA V1747, and NMMNH P-50000 is expected as those two specimens were part of the group of specimens used as coding material for the *Pentaceratops* OTU. This means when the OTU is included, MNA V1747 and NMMNH P-50000 are partially coded for twice within the analysis. Because repetition of character states in taxa weakens a tree's ability to determine relationships, including the OTU in a specimen-based analysis may have caused bias within the tree that not only affects these two specimens, but also the recovery of the other three. Consequently, a second analysis excluding the OTU was performed. The second consensus results in similar placement of MNA V1747, NMMNH P-50000, and KUVP-16100, indicating that the OTU did not have a direct impact on their recovery and their taxonomic assignment is valid. Interestingly, the OTU appears to have conflicting character states with its reference specimens.

Out of the 57 characters recorded for NMMNH P-50000, all 57 characters coded have the same states reported in the *Pentaceratops'* OTU. The 95 missing data states seem to have no effect on NMMNH P-50000 place in the *Pentaceratops* clade whether the OTU is present or not. This suggests the possibility that a large number of characters within the 152-character list are undiagnostic. MNA V1747 has 112 recorded states, the majority of which are coded based on the redescription. In the redescription, two characters are coded differently compared to the OTU: characters 53 and 149. Based upon the observations of the skull roof, the frontal contributes to the orbital margin in MNA V1747, changing character 53 from absent to present. Observations of MNA V1747's dentaries allows for coding for character 149, a lateral ridge of dentary is situated ventral to the coronoid process, as absent. The OTU records this character state as missing data due to all other reference material lacking associated lower jaws.

Because MNA V1747 is used as reference material for the OTU, characters 53 and 149 should be altered in future cladistic analyses. However, the construction of the

OTU is based upon multiple specimens with no indication of which specimen expresses which character states. Character 53 is already assigned a coded state, but because the original authors (Sampson et al., 2010) not specifying the origins of each character state, it is unclear whether or not character 53 was miscoded for the OTU, or if one of the other four specimens was used. Character 149 differs in this manner. This character is an additional character that was inserted by Mallon et al. (2011) after the construction of the OTU and is marked as missing data in subsequent studies (Mallon et al. 2011, 2014; Wick and Lehman, 2013). However, MNA V1747 has a nearly complete dentary set, so this character can be coded based upon the redescription. The rest of the redescription for MNA V1747 agrees with the coded character states used by the OTU.

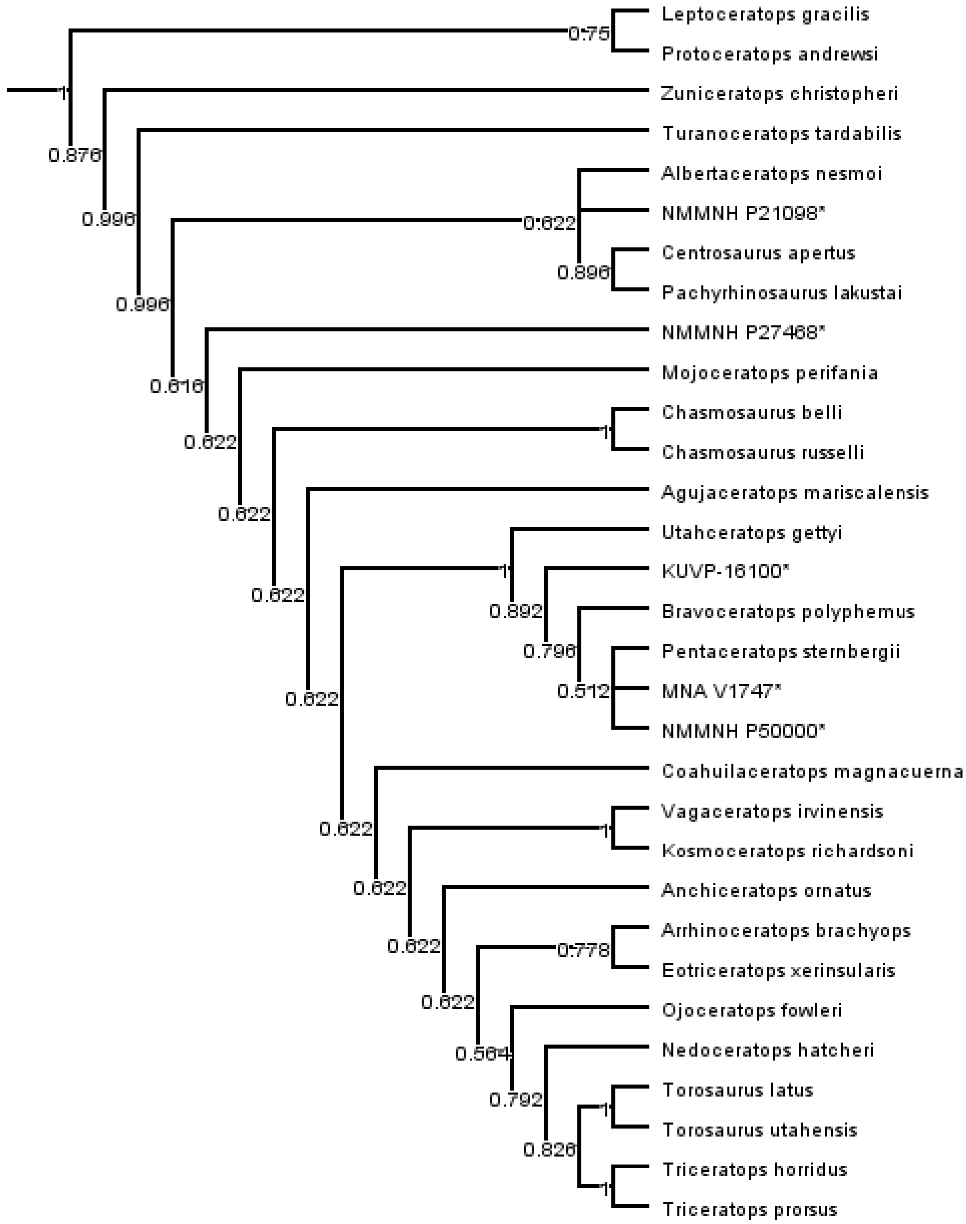

Fig. 19. Ceratopsia Majority Rules Consensus Tree. Frequency above 0.5 shown, incorporating MNA V1747, NMMNH P-21098, P-27468, P-50000, and KUVP-16100 (marked by *). TL of 311 steps, CI of 0.63, and RI of 0.754

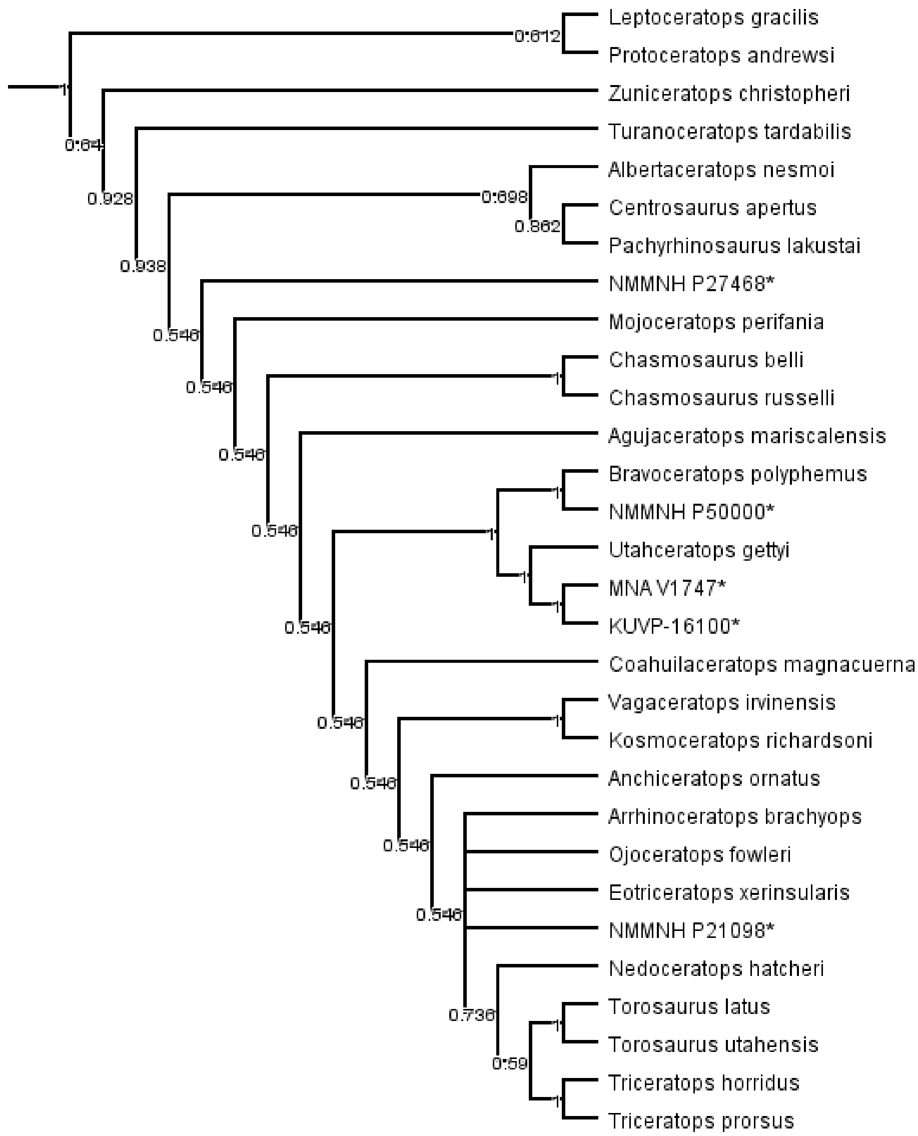

Fig. 20. Modified Majority Rules Consensus tree without *P. sternbergi*'s OTU. Frequency above 0.5 shown, incorporating MNA V1747, NMMNH P-21098, P-27468, P-50000, and KUVP-16100 (marked by *). TL of 315 steps, CI of 0.622, and RI of 0.736

KUVP-16100 has 55 coded characters with only one difference from the OTU: Character 38. Based upon observations by the author, character 38, the orientation of supraorbital horncore base, is coded as being dorsolaterally in KUVP-16100 rather than dorsally direct as seen in the OTU. KUVP-16100 is not used as reference material for the OTU meaning that any differences in character states are genuine. Because this character does not affect phylogenetic placement, the difference is likely due to intraspecific or ontogenetic variations in *Pentaceratops*, rather than evolutionary significance. Characters 38 might also be an intraspecific character in other ceratopsian taxa, which would make the character undiagnostic and lower the accuracy of the character matrix. This is only testable if other ceratopsian composite OTUs have specimens that differ from one another with regards to this character. That would require additional specimen based analyses for each taxon.

NMMNH P-27468 is recovered outside of the Pentaceratops clade in both consensus trees, rejecting the Sealey et al. (2005) assignment to *P. sternbergi*. Consequently, NMMNH P-27468 should be removed as referred material for the *P. sternbergi* OTU. Out of the 24 characters coded for NMMNH P-27468, nine character states differ from the OTU. The nine coded differences (characters 60, 64, 65, 66, 68, 97, 99, 100, and 101) are also different from the three specimens that cluster with the OTU. This implies that these differences in character states observed for NMMNH P27468 are diagnostic and distinct from different specimens of *P. sternbergi*. While this suggests that NMMNH P27468 is indeed different from *P. sternbergi,* its phylogenetic placement is unclear at this time.

Additionally, NMMNH P-27468 contains a large amount of missing data states. Mesquite, like other parsimony programs, treats missing data as reasonable and noncontroversial (Platnick et al., 1991, Wiens, 1998). Missing data, coded as"?", is treated as a "0". As a result, the number of missing characters (128) causes the phylogenetic software to treat taxa like NMMNH P27468 as basal. Prevosti and Chemisquy (2010) note that a high percentage of missing characters data in a matrix leads to a decreased the accuracy of the trees produced. Consequently, the placement of NMMNH P-27468 may be a false placement.

NMMNH P-21098 is recovered outside the *Pentaceratops* clade in both trees, but its placement differs significantly between the first consensus tree and the second consensus tree (Fig. 19 and Fig. 20). Both trees reject the taxonomic assignment by Lucas et al. (1987), Lehman (1993), and Sullivan et al. (2005) of NMMNH P- 21098 to *Pentaceratops*. With its rejection, the claim that no ceratopsian material is referable to *Pentaceratops* (Jasinski et al., 2011; Sullivan and Lucas, 2014) is now strengthened with statistical data. Additionally, NMMNH P-21098 appears to be a particularly problematic specimen. In the first tree with the OTU present, this specimen is recovered within centrosaurines, the sister group all of Chasmosaurinae (Fig. 19). When the OTU is removed (Fig. 20), NMMNH P-21098 forms a polytomy with *Ojoceratops fowleri*, *Eotriceratops xerinsularis*, and *Arrhinoceratops brachyops* and the *Triceratops* clade. This significant movement due to the removal of one taxon suggests that NMMNH P-21098 is too incomplete to determine its relationship to other ceratopsian taxa accurately.

Only 20 characters are coded for NMMNH P-21098. Of these 20, six coded characters differ from the *Pentaceratops* OTU. These six characters (character 64, 86, 87, 89, 90, and 115) differ from MNA V 1747, KUVP-16100, and NMMNH P-50000 in the same manner as the OTU. NMMNH P-21098 is not a reference material for the OTU, indicating that, as with NMMNH P-27468, the observed differences are in fact diagnostic to this specimen.

Based upon the recovery of NMMNH P21098 and NMMNH P27468, these two specimens are significantly different from *P. sternbergi* and quite possibly represent new taxa. It is noted by Mateer (1981) that multiple chasmosaurine taxa may inhabit the same stratum within the San Juan Basin (although the ceratopsian represented by NMMNH P-21098 is stratigraphically confined to the De-Na-Zin Member of the Kirtland Formation at this time). While formal descriptions and taxonomic assignment of these two specimens are outside the focus of this study, these results support a previous study

(Fowler, 2010) stating that unidentified ceratopsian taxa are present in the San Juan Basin.

Interestingly, two other ceratopsian taxa fall within the *Pentaceratops* clade (Fig. 19 and Fig. 20): *Utahceratops gettyi* and *Bravoceratops polyphemus*. In previous studies (Longrich, 2010, 2014; Sampson et al., 2010; Mallon et al. 2011, 2014; Wick and Lehman, 2013), *U. gettyi* is recovered as the sister clade to *P. sternbergi* with a strong statistical relationship (Fig .19). In the first consensus tree, *U. gettyi* is recovered as the sister group, as expected. With the removal of the OTU, *U. gettyi* falls within the Pentaceratops clade as the sister taxon to the MNA V1747 and KUVP-16100 grouping (Fig. 20). By including additional intraspecific variation for *Pentaceratops,* the results suggest that *U. gettyi* may not be a valid taxon. *U. gettyi* is based upon material from five partial specimens, meaning that its OTU is a composite like *P. sternbergi.* As seen from this study, there may be unexpected consequences when using composite OTUs. These OTU complexes can contain invalid specimens as reference material. Additionally, the use of incomplete specimens can differ significantly from their referred taxon and be misidentified for several years.

Upon closer inspection, *U. gettyi* has four character differences (characters 39, 40, 53, 68) compared to MNA V1747 and three character differences (characters 39, 40, 68) compared to KUVP-16100. Additionally, KUVP-16100 and MNA V1747 are the two stratigraphically lowest specimens in this study and *U. gettyi* is found in strata that is only slightly older that of *Pentaceratops* (Sampson et al., 2010). Both taxa are found relatively close geographically to one another. *P. sternbergi* is predominately from New Mexico with a single referred specimen from Colorado and *U. gettyi* is found only in Utah. The small morphological differences between these taxa, and the temporal and geographical proximities suggest that *U. gettyi* may be part of an anagenetic lineage with *P. sternbergi*. If this is true, *U. gettyi* should be viewed as an anagenetic precursor to *P. sternbergi,* or perhaps even referable to *P. sternbergi.*

Bravoceratops polyphemus is the other taxon that is recovered in the *Pentaceratops* clade (Fig. 19 and Fig. 20). The movement of this taxon among studies suggests a possible taxonomic issue. In the original description of *B. polyphemus*, Wick and Lehman (2013) recovered this taxon as basal to the *Triceratops* clade. In a later and cladistics analysis, Mallon et al. (2014) recovered *B. polyphemus* within a polytomy with the *Triceratops* clade, which led the authors to remove it from their other two consensus trees and to deem the taxon as problematic. Within this study, B. *polyphemus* end up within a different clade than in previous studies. This unstable placement suggests that the specimen may not be valid. *B. polyphemus* consists of an incomplete skull and has only 52 coded characters.

B. polphemus is found from the lower most part of the Javelina Formation in the Big Bend National Park, Texas (Wick and Lehman, 2013). This formation overlies the Aguja Formation, which has been correlated to the Hunter Wash Member of the Kirtland Formation (Sullivan and Lucus, 2003, 2006). Stratigraphically, *B. polphemus* is only slightly higher than the highest accepted *P. sternbergi* specimen, NMMNH P-50000 (Fig. 3). Interestingly, in the second analysis without the OTU, *B. polphemus* grouped with NMMNH P-50000 (Fig 20), and when compared to NMMNH P-50000, *B. polphemus* had only four coded character state differences (characters 37, 59, 150, and 151). It is noted though, that NMMNH P-50000 is Late Campanian while *B. polphemus* is estimated to be Late Campanian to Early Maastrichtian (Wick and Lehman, 2013). This is a larger temporal gap than between *U. gettyi* and *P. sternbergi*. These results decreases the likelihood of anagenetic linage and instead rather suggest that *B. polphemus* is mostly likely referable to *P. sternbergi*.

CONCLUSION

P. sternbergi is a large chasmosaurine ceratopsian primarily documented from the upper Fruitland and lower Kirtland formations. With the redescription of MNA V1747, several anatomical features are reported that are not seen in the original description and can be added to the taxon diagnosis. This is due to the presences of nearly complete lower jaws, both maxillae, and other facial skull elements. A detailed description of the morphology of all cranial elements suggests the modification of characters 53 (Frontal contributes to the formation of the orbit is present) and 149 (the lateral ridge ventral to the dentary is absent) in the genus' OTU. Changing these two characters in future phylogenetic studies will ensure that produced trees will reflect accurate taxonomic and evolutionary relationships.

The new description for MNA V1747 also provides comprehensive information on the most complete *P. sternbergi* found to date. This description can be used for comparing new ceratopsian specimens so taxonomic misidentification can be avoided. However, it should be noted the *P. sternbergi* holotype should be reevaluated before that any formal synonymy of possible referred taxa (such as *U. gettyi* and *B. polphemus*).

The results of the phylogenetic analyses using five referred specimens compared against the OTU and other ceratopsians indicates that only MNA V1747, NMMNH P-50000, and KUVP-16100 are confidently assigned to *P. sternbergi* (*sensu* Rowe et al., 1981). When the OTU for the genus is removed, all three specimens are still recovered within *P. sternbergi,* with the addition of *U. gettyi* and *B. polphemus*. MNA V1747 and KUVP-16100 form a grouping with *U. gettyi* while NMMNH P-50000 and *B. polphemus* form the other grouping within the clade. *B. polphemus* is a possible invalid taxon referable to *P. sternbergi* while *U. gettyi* is most likely an example of an anagenetic precursor.

The assignments of NMMNH P21098 and NMMNH P27468 to *P. sternbergi* are rejected by this study supporting previous studies/suggestions by other authors. The morphologies of these two specimens vary significantly from the *P. sternbergi's* OTU and any other referable specimen within the phylogenetic study. The results of this study indicate that multiple chasmosaurine taxa inhabit the Kirtland strata, and that the biodiversity and paleoecology of the ceratopsian taxa within the San Juan Basin is more complex than previously thought.

REFERENCES

Bauer, C.M., (1916). Contributions to the geology and paleontology of San Juan County, New Mexico: 1, Stratigraphy of a part of the Chaco River valley. *United States Geology Survey Professional Paper,* 98:274-277.

Dane, C.H., (1936). The La Ventana-Chacra Mesa coal field, Geology and fuel resources of the southern part of the San Juan Basin, New Mexico, part 3. U.*S. Geological Survey, Bulletin* 860-C, p.81-161.

Diem, S., (1999). Vertebrate faunal analysis of the Upper Cretaceous Williams Fork Formation, northwestern Colorado [M. S. thesis]: San Diego, San Diego State University, p. 188.

Diem, S. D. and Archibald, J. D., (2000). Vertebrate fauna from the Upper Cretaceous Williams Fork Formation, northwestern Colorado: *Journal of Vertebrate Paleontology*, v. 20, p. 38A-39A.

Diem, S., and Archibald, J.D., (2005). Range extension of southern chasmosaurine ceratopsian dinosaurs in northwestern Colorado: *Journal of Paleontology*, v. 79, p. 251-258.

Dodson, P., Forster, C.A., and Sampson, S.D., (2004). Ceratopsidae; In The Dinosauria, second edition. Edited by D.B. Weishampel, P. Dodson, and H. Osmólska. University of California Press, Berkeley, California. pp. 494–513.

Fassett, J. E., (1973). The saga of the Ojo Alamo Sandstone; or the rock-stratigrapher and the paleontologist should be friends. Four Corners Geological Society, Memoir Book, p. 123-130.

Fassett, J.E., (2010). Stratigraphic nomenclature of rock strata adjacent to the Cretaceous-Tertiary interface in the San Juan Basin. *New Mexico Geological Society,* 61st Field Conference, Guidebook, p. 113-124.

Fowler, D.W., (2010). Anagenesis and long-term morphologic trends in Chasmosaurinae (Dinosauria: Ceratopsidae) revealed by a new high-resolution chronostratigraphic framework, ontogenetic analysis, and description of two new taxa. *Journal of Vertebrate Paleontology*, 30 (5, abstracts volume): 91A (abstract).

Gilmore, C. W., (1916). Vertebrate faunas of the Ojo Alamo, Kirtland and Fruitland formations. U. S. Geological Survey, Professional Paper, 98Q, 279-308.

Hunt, A.P., (1986). "Bisti member" Kirtland Shale, San Juan Basin, New Mexico: implications for the basin development. *Geological Society of America*, Abstract with programs, v. 24, p. 26-27.

Hunt, A.P. and Lucas, S.G., (1992). Stratigraphy, paleontology and age of the Fruitland and Kirtland formations (Upper Cretaceous), San Juan Basin, New Mexico: *New Mexico Geological Society*, 43rd Field Conference, Guidebook, p. 217-239.

Hutchinson, P.J. and Kues, B.S., (1985). Depositional environments and paleontology of Lewis Shale to lower Kirtland Shale sequence (Upper Cretaceous), Bisti area, northwestern New Mexico: New Mexico Bureau of Mines and Mineral Resources Circular 195, p. 25-54.

Jasinski, S.E., Sullivan, R.M. and Lucas, S.G., (2011). Taxonomic composition of the Alamo Wash local fauna from the Upper Cretaceous Ojo Alamo Formation (Naashoibito Member) San Juan Basin, New Mexico: *New Mexico Museum of Natural History and Science*, Bulletin 53, p. 216-271.

Lambe, L.M., (1915). On *Eoceratops canadensis*, gen. nov., with remarks on other genera of Cretaceous horned dinosaurs. Canada *Department of Mines Geological Survey Museum Bulletin*, 12: 1–49.

Lehman, T.M., (1989). *Chasmosaurus mariscalensis*, sp., nov., a new ceratopsian dinosaur from Texas: *Journal of Vertebrate Paleontology*, v. 9, p. 137-162.

Lehman, T.M., (1990). The ceratopsian subfamily Chasmosaurinae: Sexual dimorphism and systematics; in Carpenter, K. and Currie, P. J., eds., Dinosaur systematics: Perspectives and approaches*:* Cambridge, Cambridge University Press, p. 211-229.

Lehman, T. M., (1993). New data on the ceratopsian dinosaur *Pentaceratops sternbergii* Osbornfrom New Mexico. *Journal of Paleontology, v. 67*, 279-288.

Lehman, T. M., (1998). A gigantic skull and skeleton of the horned dinosaur *Pentaceratops sternbergii* from New Mexico. *Journal of Paleontology, v. 72*, 894-906.

Longrich, N.R (2010). *Titanoceratops ouranos*, a giant horned dinosaur from the Late Campanian of New Mexico. *Cretaceous Research, 32*, 264–276.

Longrich, N. R., (2014). The horned dinosaurs *Pentaceratops* and *Kosmoceratops* from the upper Campanian of Alberta and implications for dinosaur biogeography. *Cretaceous Research*, 51, 292-308.

Lucas, S.G. and Sullivan, R.M., (2003). A new crocodylian from the Upper Cretaceous of the San Juan Basin, New Mexico: *Neues Jahrbuch für Geologie und Paläontologie*, Montashefte, 2003, p. 109-119.

Lucas, S.G., Mateer, N.J., Hunt, A.P., and O'Neill, F.M., (1987). Dinosaurs, the age of the Fruitland and Kirtland formations, and the Cretaceous-Tertiary boundary in the San Juan Basin, New Mexico. *Geological Society of America Special Paper*, 209:35-50.

Lucas, S. G., Sullivan, R .M., and Hunt, A. P., (2006). Re-evaluation of *Pentaceratops* and Chasmosaurus (Ornithischia, Ceratopsidae) in the Upper Cretaceous of the Western Interior. *New Mexico Museum of Natural History and Science, Bulletin 35*, 367-370.

Lull, R.S., (1933). A revision of Ceratopsia or horned dinosaurs. Yale Peabody Museum, Memoir 3, p. 175.

Mallon, J. C., Holmes R., Eberth D. A., Ryan, M.J., and Anderson, J. S., (2011). Variation in the skull of *Anchiceratops* (Dinosauria, Ceratopsidae) from the Horseshoe Canyon Formation (Upper Cretaceous) of Alberta. *Journal of Vertebrate Paleontology*, *v. 31,* 1047–1071.

Mallon, J. C., Holmes, R., Anderson, J. S., Farke, A. A., and Evans, D. C. (2014). New information on the rare horned dinosaur *Arrhinoceratops brachyops* (Ornithischia: Ceratopsidae) from the Upper Cretaceous of Alberta, Canada. *Canadian Journal of Earth Sciences*, 51(6), 618-634.

Marsh, O.C., (1888). A new family of horned dinosaurs from the Cretaceous. American Journal of Science, Series 3, 36: 477–478.

Marsh, O.C., (1890). Additional characters of the Ceratopsidae, with notice of new Cretaceous dinosaurs. American Journal of Science, Series 3, 39: 418–426.

Mateer, N.J., (1981). The reptilian mega-fauna from the Kirtland Shale (Late Cretaceous) of the San Juan Basin, New Mexico. In S. Lucas, K. Rigby, and B. Kues (eds.), Advances in San Juan Basin Paleontology. University of New Mexico Press, Albuquerque, New Mexico.

Osborn, H. F., (1923). A new genus and species of Ceratopsia from New Mexico. *American Museum Novitates, no. 93*, 1-3.

Owen, R., (1842). Report on British fossil reptiles. Part II. Report of the British *Association for the Advancement of Science*, pp. 60–204.

Prevosti, F.J., and Chemisquy, M.A., (2010). The impact of missing data on real morphological phylogenies: influence of the number and distribution of missing entries. *Cladistics*, 26(3), p. 326-339.

Platnick, N. I., Griswold, C. E., and Coddington, J. A., (1991). On missing entries in cladistic analysis. *Cladistics*, 7(4), 337-343.

Reeside, J.B., Jr., (1924).Upper Cretaceous and Tertiary formations of the western part of the San Juan Basin of Colorado and New Mexico. U.S. Geological Survey Professional Paper, 134, p.1-70.

Rowe, T.E., Colbert, H., and Nations, J.D., (1981). The occurrence of *Pentaceratops*(Ornithischia: Ceratopsia) with a description of its frill. In S. Lucas, K. Rigby, and B. Kues (Eds.), *Advances in San Juan Basin Paleontology* (pp. 29-48). University of New Mexico Press, Albuquerque.

Sampson, S.D., Loewen, M.A., Farke, A.A., Roberts, E.M., Forster, C.A., Smith, J.A., and Titus, A.L., (2010). New horned dinosaurs from Utah provide evidence for intracontinental dinosaur endemism. PLoS ONE, 5(9): e12292.

Sealey, P., Smith, J., and Williamson, T., (2005). An unusual *Pentaceratops* from New Mexico. *Journal of Vertebrate Paleontology*, 25(3) p. 113A (abstract).

Seeley, H.G., (1887). On the classification of the fossil animals commonly named Dinosauria. Proceedings of the Royal Society of London, 43: 165–171.

Swofford. D.L., (1993). PAUP: Phylogenetic analysis using parsimony, version 3.1. *Programme and documentation*. Washington, DC: Smithsonian Institution.

Sullivan, R.M. and Lucas, S.G., (2003). The Kirtlandian, a new land-vertebrate "age" for the Late Cretaceous of Western North America: *New Mexico Geological Society*, 54th Field Conference, Guidebook, p. 369-377.

Sullivan, R.M., and Lucas, S.G., (2010). A new chasmosaurine (Ceratopsidae, Dinosauria) from the Upper Cretaceous Ojo Alamo Formation (Naashoibito Member), San Juan Basin, New Mexico. New perspectives on horned dinosaurs (pp. 169-180). In M.J. Ryan, B.J. Chinnery-Allgeier, and DA Eberth (eds), Indiana University Press, Bloomington, Indiana.

Sullivan, R.M., and Lucas, S.G., (2014). Stratigraphic distribution of Hadrosaurids in the Upper Cretaceous Fruitland, Kirtland, and Ojo Alamo formations, San Juan Basin, New Mexico; in Eberth, D.A. and Evans,D.E., eds., Hadrosaurs; Bloomington, Indiana University Press.

Sullivan, R.M., and Lucas, S.G., (2015). C.H. Sternberg's 1921 Uppsala (Museum of Evolution) *Pentaceratops* skeleton quarry located. *New Mexico Museum of Natural History and Science, Bulletin 67*, 383-388.

Sullivan, R.M., and Lucas, S.G., (in press). Cretaceous Vertebrates of New Mexico.

Sullivan, R.M., Boere, A.C., and Lucas, S.G., (2005). Redescription of the ceratopsid dinosaur *Torosaurus utahensis* (Gilmore, 1946) and a revision of the genus. *Journal of Paleontology, v* 79, p. 283-288.

Wick, S.L., and Lehman, T.M., (2013). A new ceratopsian dinosaur from the Javelina Formation (Maastrichtian) of West Texas and implications for chasmosaurine phylogeny. *Naturwissenschaften*, v.100: 667–682.

Wiens, J. J., (1998). Does adding characters with missing data increase or decrease phylogenetic accuracy?. *Systematic Biology*, v.47, 625-640.

Wiman, C., (1930). Uber Ceratopsia aus der obern Kreide in New Mexico. *Nova Acta Regiae Societatis Scientiarum Upsaliensis, series* 4, 7:1-19.

APPENDIX

Character states are scored for MNA V1747, NMMNH P-21098, NMMNH P-27468, NMMNH P-50000 and KUVP-16100 using 148 characters given by Sampson et al. (2010), including an two additional characters (149, 152) described by Mallon et al. (2011,2014) respectively and two additional characters (150, 151) described by Wick and Lehman (2013). The following changes were made to the modified Mallon et al. (2014) matrix: *P. sternbergi* 53(0), 149 (1).

Phylogenetic Analysis: Specimens Included. Specimens and literature sources used for the scoring of taxa in the phylogenetic analysis. **AMNH**, American Museum of Natural History, New York NY; **ANSP**, Academy of Natural Sciences of Philadelphia, Philadelphia, PA; **CMN**, Canadian Museum of Nature (formerly National Museum of Canada), Ottawa, Ontario, Canada; **CPS**, Colección Paleontológica de Coahuila, at the Museo del Desierto, Saltillo, Coahuila, Mexico; **IGM**, Mongolian Institute of Geology, Ulaan Bataar, Mongolia; **KUVP** (formerly known as UKVP), University of Kansas Natural History Museum, Lawrence**,** KS; **LACM**, Los Angeles County Museum, Los Angeles, CA; **MNA**, Museum of Northern Arizona, Flagstaff, AZ; **MSM**, Mesa Southwest Museum, Mesa, AZ; **NMMNH**, New Mexico Museum of Natural History, Albuquerque, NM; **ROM**, Royal Ontario Museum, Toronto, Ontario Canada; **SMP**, State Museum of Pennsylvania, Harrisburg, PA; **TMM**, Texas Memorial Museum, University of Texas at Austin, Austin, TX; **TMP**, Royal Tyrell Museum of Paleontology, Drumheller, Alberta, Canada; **UALVP**, University of Alberta Laboratory of Vertebrate Paleontology, Edmonton, Alberta, Canada; **UMNH VP**, Utah Museum of Natural History, Salt Lake City, Utah; **USNM**, National Museum of Natural History, Smithsonian Institute, Washington, DC; **UTEP**, University of Texas El Paso, currently at **TMM**; **YPM**, Peabody Museum, Yale University, New Haven, CT.

Taxa List

Taxon	**Source**
Leptoceratops gracilis:	CMN 8887, 8889
Protoceratops andrewsi:	AMNH and IGM various specimens
Turanoceratops tardabilis:	Sues and Averianov, 2009; Farke et al., 2009
Zuniceratops christopheri:	MSM bonebed specimens
Albertaceratops nesmoi:	TMP 2001.26.01
Centrosaurus apertus:	CMN 348, 8798, 8795; ROM 878; UALVP 11735.
Pachyrhinosaurus lakustai:	TMP 86.55.258, 87.55.156, 89.55.1234
Chasmosaurus belli:	CMN 2245, ROM 843
Chasmosaurus russelli:	CMN 2280, 8800
Mojoceratops perifania:	AMNH 5401, 5656; TMP 83.25.1
Agujaceratops mariscalensis:	TMM 43098-1 and UTEP bonebed specimens
Utahceratops gettyi:	UMNH VP 12198, 12225, 13919, 16671, 16673-75
Pentaceratops sternbergi:	AMNH 1624,6324; MNA 1747; NMMNH P-27468, 50000
Coahuillaceratops magnacuerna:	CPS 276, CPS 277
Vagaceratops irvinensis:	CMN 41357; TMP 87.45.1, 98.102.8
Kosmoceratops richardsoni:	UMNH VP 12198, UMNH VP 14523
Vagaceratops irvinensis:	CMN 4135; TMP 87.45.1, TMP 98.102.8
Anchiceratops ornatus:	AMNH 5251, 5273; CMN 8535; TMP 83.01.01
Arrhinoceratops brachyops:	ROM 796, ROM 1439
Ojoceratops fowleri:	SMP VP-1575, VP-1828, VP-1719, VP-1828, VP-1865, VP-1875, VP-2090, and other specimens; NMMNH P-4447
Torosaurus latus:	ANSP 15192; MOR 980, 1122; YPM 1830, 1831
Torosaurus utahensis:	USNM 15583, 15875, 15887, 16168, 16573-4, 16576

Eotriceratops xerinsularis:	TMP 2002.57.7
Nedoceratops hatcheri:	USNM 2412
Triceratops horridus:	USNM 1201, 1205, 2100; YPM 1820, 1821
Triceratops prorsus:	LACM 7303, 27428; YPM 1822

MNA V1747
NMMNH P-21098
NMMNH P-27468
NMMNH P-50000
KUVP-16100

Character List

[1] 'Rostral, extent of dorsal and ventral processes(Dodson et al., 2004, character 1)'
[2] 'Nares, size and position (Sereno, 1999, characters 106-108, modified)'
[3] 'Premaxillary septum (Chinnery and Weishampel, 1998, character 10)'
[4] 'Premaxillary septum, shape (Dodson et al., 2004, character 4)'
[5] 'Premaxillary septum, nasal contribution (Sampson et al., 2010)'
[6] 'Premaxilla, narial strut (Holmes et al., 2001, character 1)'
[7] 'Premaxilla, narial strut orientation (Dodson et al., 2004, character 6)'
[8] 'Premaxilla, septal flange (Holmes et al., 2001, character 2)'
[9] 'Premaxilla, septal flange length (Forster et al., 1993, character 1)'
[10] 'Premaxilla, septal fossa (Holmes et al., 2001, character 4)'
[11] 'Premaxilla, interpremaxillary fossa in premaxillary septum (Dodson et al., 2004, character 8)'
[12] 'Premaxilla, accessory strut in septal fossa (Sampson et al., 2010)'
[13] 'Premaxilla, triangular process (Forster, 1990, character 21)'
[14] 'Premaxilla, triangular process shape (Sampson et al., 2010)'
[15] 'Premaxilla, triangular process recess (Dodson et al., 2004, character 12)'
[16] 'Premaxilla, recess along ventral portion of septum (Dodson et al., 2004, character 9)'
[17] 'Premaxilla, caudoventral expansion of oral margin (Forster, 1990, character 6)'
[18] 'Premaxilla, position of caudal tip of caudoventral process (Forster et al., 1993, character 7)'
[19] 'Premaxilla, distal end of caudoventral process forked (Forster, 1990, character 14)'
[20] 'Premaxilla-nasal contact in dorsal view (Sampson et al., 2010)'
[21] 'Accessory antorbital fenestra (Forster, 1990, character 15)'
[22] 'Accessory antorbital fenestra size (Sampson et al., 2010)'
[23] 'External antorbital fossa, size (Forster, 1990, character 44)'
[24] 'Maxilla, relation of alveolar margin to rostral edentulous margin (Sampson et al., 2010)'
[25] 'Maxilla, diastema on rostral maxilla (Sampson et al., 2010)'
[26] 'Maxilla, maxillary cavity (Sampson et al., 2010)'
[27] 'Nasal, ornamentation in adult (Forster, 1990, character 26, 27, 28, 126, modified)'
[28] 'Nasal, ornamentation type in adult (ORDERED) (Forster, 1990, character 26, 27, 28, 126, modified)'
[29] 'Nasal, ornamentation position, measured perpendicular to a horizontal toothrow (Forster, 1990, character 29, modified)'
[30] 'Nasal, narial spine (Forster, 1990, character 22)'

[31] 'Facial skeleton, dorsoventral depth in orbital region (Sampson et al., 2010)'
[32] 'Orbit, orientation (Sampson et al., 2010)'
[33] 'Orbit diameter (Makovicky & Norell, 2006, character 3, modified)'
[34] 'Lacrimal, size (Chinnery and Weishampel, 1998, character 1)'
[35] 'Postorbital, supraorbital ornamentation in adult (Forster, 1990, characters 56 and 57, modified)'
[36] 'Postorbital, extent of cornual sinuses in base of supraorbital ornamentation (Forster, 1990, character 123, modified)'
[37] 'Postorbital, position of supraorbital horncore (Lehman, 1996, character 9)'
[38] 'Postorbital, orientation of supraorbital horncore base (Sampson et al., 2010)'
[39] 'Postorbital, length of supraorbital horncore (Forster, 1990, character 58, modified)'
[40] 'Postorbital, curvature of supraorbital horncore in lateral view (Forster et al., 1993, character 2, modified)'
[41] 'Postorbital, curvature of supraorbital horncore in rostral view (Sampson et al., 2010)'
[42] 'Postorbital, separation from laterotemporal fenestra (Makovicky & Norell, 2006, character 34, modified)'
[43] 'Palpebral, shape (Forster, 1990, character 31, modified)'
[44] 'Palpebral, antorbital buttress (Sampson, 1995, character 7, modified)'
[45] 'Palpebral, extent of antorbital buttress (Sampson et al., 2010)'
[46] 'Jugal, size and orientation of jugal body (Makovicky, 2001, character 22)'
[47] 'Jugal infratemporal process (Forster, 1990, character 62, modified)'
[48] 'Jugal-lacrimal contact (Makovicky and Norell, 2006, character 26)'
[49] 'Epijugal attachment scar (Sereno 1999, character 113, modified)'
[50] 'Epijugal length (Sampson et al., 2010)'
[51] 'Quadratojugal-squamosal contact (Sampson et al., 2010)'
[52] 'Laterotemporal fenestra, size and position (Chinnery and Weishampel, 1998, character 7)'
[53] 'Frontal, contribution to orbital margin (Forster, 1990, character 51)'
[54] 'Frontal, contribution to dorsotemporal fenestra (Sampson et al., 2010)'
[55] 'Frontal fontanelle leading into supracranial cavity complex (Forster et al., 1996, character 3, modified)'
[56] 'Frontal fontanelle, shape (Forster, 1990, characters 49 and 50, modified)'
[57] 'Parietal, anterior extent on dorsum of skull relative to occipital condyle (Sampson et al., 2010)'
[58] 'Squamosal, posterior expansion (Sampson et al., 2010)'
[59] 'Squamosal, shape of expanded blade (Sampson et al., 2010)'
[60] 'Squamosal, length relative to parietal (Holmes et al., 2001, character 19, modified)'

[61] 'Squamosal forms part of posterior margin of frill (Sampson et al., 2010)'
[62] 'Squamosal, rostromedial lamina forming the caudolateral floor of dorsotemporal (Penkalski and Dodson, 1999, character 9)'
[63] 'Squamosal-quadrate contact (Forster, 1990, character 64, modified)'
[64] 'Squamosal, thickened, rounded swelling along medial margin (Forster, 1990, character 90)'
[65] 'Parietosquamosal contact, shape in lateral view (Sampson et al., 2010) (Forster, 1990, character 119)'
[66] 'Parietal, concave median embayment on caudal margin (Sampson et al., 2010)'
[67] 'Parietal, shape of concave median embayment (Forster, 1990, character 83, modified) PROBLEM WITH NUMBERS ON SHEET'
[68] 'Parietal, location of caudalmost point of caudal ramus (Holmes et al., 2001, character 18, modified)'
[69] 'Parietosquamosal frill, length relative to basal skull length (Forster, 1990, characters 80, 81, 82, modified)'
[70] 'Parietosquamosal frill, location of maximum transverse width (Sampson et al., 2010)'
[71] 'Parietal, parietal sulci (Sampson et al., 2010)'
[72] 'Parietal, overall shape (Sampson et al., 2010)'
[73] 'Parietal fenestra (Forster, 1990, character 84) '
[74] 'Parietal, rim on medial margin of dorsotemporal fenestra (Forster, 1990, character 86). CORRECTED.'
[75] 'Parietal, sharp median crest (Sampson et al., 2010)'
[76] 'Parietal, rostrocaudal thickness of transverse bar at narrowest point (Holmes et al., 2001, character 22)'
[77] 'Parietal, relative rostrocaudal depth of broad transverse bar (Sampson et al., 2010)'
[78] 'Parietal, cross-sectional shape of median bar (Holmes et al., 2001, character 24, modified)'
[79] 'Parietal, median bar, transverse width (Holmes et al., 2001, character 23)'
[80] 'Parietal fenestra, orientation (Forster, 1990, character 129, modified) CORRECTED'
[81] 'Parietal fenestra, maximum proximodistal diameter (Forster, 1990, character 129, modified)'
[82] 'Parietosquamosal frill, marginal undulations (Forster, 1990, characters 89, 114, modified)'
[83] 'Parietosquamosal frill, imbrication of undulations (Dodson et al., 2004, character 34)'

[84] 'Marginal dermal ossifications on parietal and squamosal (Forster, 1990, characters 91 and 92, modified)'
[85] 'Episquamosals on midlateral squamosal margin (Sampson et al., 2010)'
[86] 'Episquamosal, location of largest/longest example (Sampson et al., 2010)'
[87] 'Episquamosal, midlateral, shape (Dodson et al., 2004, character 45, modified)'
[88] 'Episquamosal locus S1 shape (Sampson et al., 2010)'
[89] 'Episquamosal locus S2 shape (Sampson et al., 2010)'
[90] 'Episquamosal locus S2 size relative to other episquamosals (Sampson et al., 2010)'
[91] 'Marginal ossification crossing squamosal-parietal contact (Dodson et al., 2004, character 43)'
[92] 'Shape of marginal ossification crossing squamosal-parietal contact (Sampson et al., 2010)'
[93] 'Epiparietals, number per side (Holmes et al., 2001, character 28)'
[94] 'Epiparietals, fused to adjacent epiparietal at base (Holmes et al., 2001, character 29)'
[95] 'Epiparietal P0 (Sampson et al., 2010)'
[96] 'Epiparietal locus DPP1 (Sampson, 1995, character 14, modified)'
[97] 'Epiparietal, locus P1 shape (Sampson, 1995, character 15, modified)'
[98] 'Epiparietal, locus P1 orientation (Sampson, 1995, character 15, modified)'
[99] 'Epiparietal, locus P1 curvature (Sampson, 1995, character 15, modified)'
[100] 'Epiparietal, locus P2 shape (Sampson, 1995, character 16, modified)'
[101] 'Epiparietal, locus P2 curvature (Sampson, 1995, character 16, modified)'
[102] 'Epiparietal locus P3 shape (Sampson et al., 2010)'
[103] 'Epiparietal, locus P3 orientation (Sampson et al., 2010)'
[104] 'Basioccipital,contribution to occipital condyle (Forster, 1990, character 71)'
[105] 'Supraoccipital, contribution to foramen magnum (Forster, 1990, character 63)'
[106] 'Supraoccipital, ventrolateral processes (Sereno, 1999, character 131)'
[107] 'Exoccipital, exits for cranial nerves in exoccipital (Forster, 1990, character 68)'
[108] 'Paroccipital process, dorsoventral distal expansion (Forster, 1990, character 66)'
[109] 'Ectopterygoid, contributes to palate and contacts the jugal (Forster, 1990, character 32)'
[110] 'Secondary palate, relative contribution of maxilla (Sampson et al., 2010)'
[111] 'Palatine, shape and relationship to maxilla (Sampson et al., 2010)'
[112] 'Lower jaw, level of mandibular articulation (Forster, 1990, character 74)'
[113] 'Predentary, length relative to dentary (Chinnery, 1998, character 19; polarity reversed)'
[114] 'Predentary, dentary processes (Sampson et al., 2010)'
[115] 'Predentary, orientation of triturating surface (Dodson, 2004, character 57)'

[116] 'Dentary lateral ridge confluent with cutting surface of predentary (Sampson et al., 2010)'
[117] 'Dentary, shape of ventral margin in adults (Forster, 1990, character 73)'
[118] 'Dentary, caudal extent of tooth row (Chinnery and Weishampel, 1998, character 18)'
[119] 'Dentary, shape of coronoid process (Forster, 1990, characters 33 and 72, modified)'
[120] 'Dentary, separation of body from ascending ramus of coronoid process (Makovicky, 2001, character 59, modified)'
[121] 'Splenial, shape (Makovicky, 2001, character 62, modified)'
[122] 'Prearticular-dentary contact (Sampson et al., 2010)'
[123] 'Tooth, number of roots (Forster, 1990, character 34)'
[124] 'Tooth, number of replacements per alveolus (Sereno, 1999, character 137)'
[125] 'Tooth magazine, case-like alveolar slots for vertical tooth families formed by spongy bone (Sampson et al., 2010)'
[126] 'Cheek teeth (Forster, 1990, character 37)'
[127] 'Cervical vertebrae, formation of syncervical (Forster, 1990, character 122)'
[128] 'Axis, neural spine shape and orientation (Sereno, 1999, character 141)'
[129] 'Atlantal rib (Sampson et al., 2010)'
[130] 'Dorsal vertebrae, shape of centra (Sampson et al., 2010)'
[131] 'Sacrum, longitudinal sulcus on ventral surface (Lehman, 1989; Sereno, 1999, character 144)'
[132] 'Scapula, relative contribution to glenoid fossa (Sereno, 1999, character 145)'
[133] 'Scapula, orientation of scapular spine (Sampson et al., 2010)'
[134] 'Olecranon process (Forster, 1990, character 104, modified)'
[135] 'Clavicle (Sereno, 1999, character 147)'
[136] 'Manual and pedal unguals, shape (Chinnery and Weishampel, 1998, character 64)'
[137] 'Manal and pedal penultimate phalanges, shape (Sampson et al., 2010)'
[138] 'Ilium, lateral eversion of dorsal margin (Forster, 1990, characters 108-109, modified)'
[139] 'Ilium, relative lengths of pubic and ischial peduncles (Sampson et al., 2010)'
[140] 'Pubis, prepubic process (Forster, 1990, character 111)'
[141] 'Pubis, position and length of postpubic rod (Forster, 1990, character 110)'
[142] 'Pubis and ischium, morphology of contributions to acetabulum (Sampson et al., 2010)'
[143] 'Ischium, cross-sectional shape of shaft (Forster, 1990, character 112)'
[144] 'Ischium, orientation of shaft (Forster, 1990, character 113)'

[145] 'Femur, morphology of greater and lesser trochanters (Dodson et al., 2004, character 72)'
[146] 'Femur, size of fourth trochanter (Sereno, 1999, character 154)'
[147] 'Femur-tibia proportion (Forster, 1990, character 103)'
[148] 'Pes, metatarsal proportions (Sampson et al., 2010)'
[149] 'Lateral ridge of dentary, situated ventral to the coronoid process (Mallon et al., 2011)'
[150] 'Form of the quadratojugal-squamosal joint in lateral view (Wick and Lehman et al., 2013)'
[151] 'Form of the nasal bridge in dorsal view (Mallon et al., 2014)'
[152] 'Nasal horncore transverse cross-section (Mallon et al., 2014)'

State Labels {(0/1) or (0/1/2) etc.}

1. 'triangular in lateral view, with short dorsal and ventral processes'/'elongate, with deeply concave caudal margin and hypertrophied dorsal and ventral processes'
2. 'small, restricted to dorsal 1/3 of premaxilla, undifferentiated, 10% or less that of basal skull length'/'large, expanded to occupy most of the depth of the premaxilla, 15% or greater than basal skull length'
3. absent/present,
4. 'rostrally elongate'/hemicircular,
5. 'septum formed by premaxilla only'/'septum formed by premaxilla and nasal',
6. absent/ present,
7. 'rostrally inclined'/'caudally inclined',
8. absent/ present,
9. 'spans entire caudal margin of narial strut'/'restricted to ventral portion of narial strut',
10. absent/present,
11. absent/ present,
12. 'no accessory strut'/'strut present',
13. absent/ present,
14. square/ 'pinched and triangular with concave facets',
15. absent/present,
16. absent/present,
17. absent/ present,
18. 'inserts into an embayment in the nasal'/'intervenes between nasal and maxilla',
19. absent/present,
20. 'premaxillae insert between nasal'/'nasals insert between premaxillae',
21. present/absent,
22. 'pronounced, penetration of nasal cavity visible in lateral view'/'slight penetration, nasal cavity not visible in lateral view',
23. 'large, 20% or more length of body of maxilla'/'greatly reduced or absent, less than 10% length of body of maxilla',
24. 'edentulous portion maxilla elevated above level of alveoli'/'at same level',
25. present/absent,
26. absent/ present,
27. absent/ present,
28. 'non-pronounced'/'distinct horncore'/'pachyostotic boss',
29. 'centered dorsal to or caudal to center of endonaris'/'centered rostal to center of endonaris',

30. absent/ present,
31. 'deep, alveolar process of maxilla entirely visible'/'shallow, alveolar process of maxilla obscured by jugal',
32. 'directed rostrolaterally'/'directed laterally',
33. 'more than 20% of skull length'/'less than 15% of skull length',
34. 'large, forms 50% or more of the rostral orbital margin'/'small, forms 40% or less of the rostral orbital',
35. absent/ present,
36. 'sinus space invades frontal and parietal'/'sinus space enters postorbital',
37. 'centered rostrodorsal or dorsal to orbit, narrow base with caudal margin of supraorbital horncore extending to or only slightly behind caudal margin of orbit'/'centered caudodorsal to orbit, broad base with caudal margin of supraorbital horncore extending well behind caudal orbit',
38. 'dorsally directed'/'dorsolaterally directed',
39. 'short, less than 15% basal skull length'/'present, elongate, greater than 35% basal skull length',
40. 'caudally recurved'/'rostrally curved'/straight,
41. 'medially recurved'/'laterally curved'/ straight,
42. 'narrowly excluded from fenestra by narrow strip of jugal'/'broadly excluded from fenestra by a substantial jugal-squamosal contact ',
43. 'rod-like, articulates with prefrontal only at its base and projects across dorsal orbit, ligamentous attachment'/'blocky, fully fused into dorsal orbital margin, sutural articulation with prefrontal and frontal ',
44. 'absent '/'present ',
45. 'present along only anterodorsal portion of orbit '/'present along entire anterior portion of orbit ',
46. 'projects strongly caudoventrally, does not extend below the level of the maxillary tooth row '/'projects nearly ventrally, elongated to extend below the level of the maxillary tooth row ',
47. 'absent '/'present, contacts or nearly contacts infratemporal process of squamosal ',
48. 'reduced '/'expanded ',
49. 'large blade like triangle with obtuse angle oriented towards quadratojugal '/'scar roughly equilateral in shape ',
50. 'long '/'hyperlong '/short,
51. 'absent '/'present ',
52. 'relatively large, diameter 20% or greater that of basal skull length, positioned caudal to orbit '/'greatly reduced, diameter 10% or less that of basal skull length, positioned entirely below ventral limit of orbit ',

53. 'present '/'absent ',
54. 'present '/'absent ',
55. 'absent '/'present ',
56. 'transversely narrow, slit-like '/'key-hole shaped, circular or elongate oval ',
57. 'rostral end of parietal located well in front of occipital condyle '/'rostral end of parietal lies directly over occipital condyle ',
58. 'absent or very slight '/'present ',
59. 'sub-rectangular in outline '/'triangular in outline, posteriorly narrowed ',
60. 'squamosal much shorter than parietal, large portion of posterolateral frill made up of parietal '/'squamosal slightly shorter than parietal, pmn;y posterolaterl-most margin of frill formed by the parietal '/'squamosal and parietal equal in length',
61. 'present '/'absent ',
62. 'absent '/'present ',
63. 'socket-like cotylus on ventrolateral squamosal for ball-like quadrate head '/'elongate groove on medial surface of squamosal to receive lamina of quadrate ',
64. 'absent, lateral surface of squamosal flat to slightly convex '/'present, lateral surface of squamosal slightly concave ',
65. 'straight '/'curved, medially concave ',
66. 'absent '/'present ',
67. 'shallow, restricted to center of margin '/'shallow, entire transverse bar is a V-shaped embayment '/'notch-like, restricted to center of margin',
68. 'on midline '/'between midline and lateral-most corner '/'at lateral-most corner adjacent to squamosal',
69. 'short, .70 or less '/'elongate, .85 or more ',/
70. 'caudally, at rear margin of frill '/'rostrally, in association with proximal half of frill '/'widest part in middle or frill relatively equal in width',
71. 'absent '/'present ',
72. 'nearly straight along midline in lateral view and gently arched from side to side '/' "saddle-shaped," dorsally concave in lateral view with upturned caudal margin, and arched strongly from side to side ',
73. 'absent '/'present ',
74. 'absent /'present, well-defined, laterally projecting rim defines medial margin of fenestra ',
75. 'present '/'absent ',
76. 'narrow and straplike, less than 10% total parietal length '/'broad, 20% or more of total parietal length ',
77. 'subequal medial to lateral '/'tapering so that the narrowest point occurs medially ',

78. 'diamond-shaped, tapers laterally '/'rectangular or subrectangular, margin facing parietal fenestrae thick and oriented sub-perpendicular to parietal surface '/ 'round to lenticular'/'v-shaped, opening ventrally',
79. 'narrow and straplike, transverse width less than 10% total parietal length '/'relatively wide, transverse width 15% or more of total parietal length ',
80. 'long axis directed transversely '/'long axis directed axially '/'axial and transverse axes equal',
81. '35% or less total parietal length '/'45% or more total parietal length ',
82. 'absent '/'present ',
83. 'absent '/'present ',
84. 'absent '/'present ',
85. 'small, less than 50 mm long in adults '/'large and elongate, greater than 90mm long in adults ',
86. 'episquamosals subequal in size '/'rostralmost episquamosal by far the largest '/'caudalmost episquamosal by far the largest',
87. 'crescentic or ellipsoidal '/'triangular or elongate ',
88. 'small and crescentic '/'low raised D-shaped process '/'well developed larger triangular process'/'elongate hook',
89. 'small and crescentic '/'low raised D-shaped process '/'well developed larger triangular process',
90. 'subequal '/'second only to S1 in size, larger than S3 ',
91. absent/present,
92. 'small and crescentic '/'present strongly recurved process or gnarled process '/'well developed triangular process sometimes with a small peak',
93. 'three '/ 'five or more ',
94. 'absent '/'present ',
95. 'absent '/'present ',
96. 'absent '/”present ',
97. 'low D-shaped process '/'elongate flattened process or spike '/'strongly recurved triangular or recurved low gnarled triangular process'/'well developed triangular process'/'elongate low process sometimes with a small peak',
98. 'caudally, epiparietal oriented in the plane of the frill '/'directed rostrodorsally '/'P1 occurs on dorsal surface of parietal',
99. 'straight '/'laterally curved ,'/'medially curved'/'dorsally curved',
100. 'low D-shaped process '/'elongate flattened process or spike '/'strongly recurved triangular or recurved low gnarled triangular process'/'well developed triangular process'/'elongate low process sometimes with a small peak',

101. 'straight '/'medially or laterally curved in the plane of the frill '/'recurved onto dorsal surface of frill',
102. 'low raised D-shaped process '/'elongate spike '/'strongly recurved triangular or recurved low gnarled triangular process'/'well developed triangular process'/'elongate low process sometimes with a small peak',
103. 'caudally, epiparietal oriented in the plane of the frill '/'directed rostrodorsally ',
104. 'forms approximately 2/3 of occipital condyle '/'forms 1/3 of the occipital condyle',
105. 'forms dorsal margin of foramen magnum ','eliminated from margin by exoccipital-exoccipital contact on midline ',
106. 'absent '/'present ',
107. 'three foramina '/'two foramina ',
108. 'distal process only slightly expanded '/'distal process expanded to at least .8 two times the depth at its narrowest point ',
109. 'present '/'absent ',
110. 'maxilla forms at least 45% of the secondary palate '/'maxilla contributes only to the posterior portion, forms 30% or less of secondary palate ',
111. 'palatine contacts nearly the entire medial surface of the maxilla, restricting size of choanae, rostrodorsal process embraces posterior end of vomer ''palatine contacts only the posterior one-third of medial surface of maxilla, contact with vomer lost, choanae enlarged ',
112. 'at or slightly below occlusal surface of tooth row '/'depressed well below level of occlusal surface of tooth row ',
113. 'equal to or more than two-thirds of dentary length '/ 'less than two-thirds of dentary length ',
114. 'ventral processes much longer than abbreviated dorsal processes '/'dorsal and ventral processes elongate and subequal in length ',
115. 'nearly horizontal '/'inclined steeply laterally',
116. 'present '/'absent ',
117. 'strongly convexly bowed '/'straight ',
118. 'terminates at the center of the coronoid process '/'terminates caudal to the coronoid process ',
119. 'short, with gently convex apex, base of ascending ramus rostrocaudally expanded/'tall, expanded at apex into a rostrally projecting hook, base of ascending ramus rostrocaudally restricted ',
120. 'absent '/'present ',
121. 'nearly as deep as the body of the dentary, does not contact articular, angular exposed in medial view '/'shallow, contacts articular, covers angular in medial view ',

122. 'absent '/'present ',
123. 'one '/'two ',
124. 'one or two replacement teeth'/'three or more replacement teeth ',
125. 'absent '/'present ',
126. 'spaced ''closely packed, roots abut ',
127. C1-3 fused or tightly articulated, atlantal hypocentrum present as a ventrally placed, wedge-like bone '/'C1-3 firmly fused, atlantal hypocentrum forms a complete ring',
128. 'blade-like and nearly vertical, overhangs only rostralmost portion of C3 '/'blade-like morphology lost, spine steeply angled to reach caudal margin of C3 ',
129. 'present '/'absent ',
130. 'relatively axially elongate ''axially shortened ',
131. 'absent '/'present '
132. 'scapula and coracoid contribute equally ','scapula contributes well over half of the glenoid ',
133. 'runs obliquely across blade '/ 'runs longitudinally along blade ',
134. 'relatively small '/'enlarged (>one-third of ulnar length) ',
135. 'present '/'absent ',
136. 'taper to distal tip '/'dorsoventrally flattened with blunt and rounded distal tips ',
137. 'length exceeds width '/'width exceeds length',
138. 'absent '/'present ',
139. 'pubic and ischial peduncles long, extend well below body of ilium approximately the same distance '/'ischial peduncle reduced along ventral aspect, pubic peduncle projects further ventrally than ischial peduncle ',
140. 'short and unexpanded distally '/'elongate, distal end greatly expanded dorsoventrally '
141. 'relatively short but extends past ischial peduncle of ilium, arises ventral to acetabulum and lies along ventral and ventromedial margin of ischium '/'very abbreviated, terminates at level of ischial peduncle, arises medial to acetabulum and passes entirely medial to ischium ',
142. 'pubic acetabular surface faces caudolaterally, pubis and pubic process of ischium contribute equally to ventral margin of acetabulum '/'pubic acetabular surface faces laterally and forms a partial medial wall to the acetabulum, pubic process of ischium elongate and meets pubis close to anterior margin of acetabulum, ventral portion of pubic acetabular surface lies medial to pubic ramus of ',
143. 'thick and ovoid '/'laterally compressed and bladelike, tapered dorsally ',
144. 'nearly straight or slightly decurved '/ 'broadly and continuously curved ',

145. 'trochanters distinct and located below the level of the femoral head '/'trochanters coalesced and level with the femoral head ',
146. large and pendant '/'small, reduced to low prominence ',
147. 'tibia longer than femur '/'femur longer than tibia ',
148. 'length of MT I two-thirds the length of MT II '/'MT I reduced to one half or less the length of MT II ',
149. present/absent,
150. 'quadratojugal overlapped by squamosal dorsally '/'quadratojugal bifurcated with processes dorsal and ventral to squamosal ',
151. 'wide posterior to the nasal horncore '/'constricted posterior to the nasal horncore ',
152. Ellipse- or teardrop-shaped'/'Triangular (horncore with flattened rostral face and distinct caudal keel)',

Matrix

Leptoceratops_gracilis
100??0???0??0??010001?000?0??000000??????000?0000000000?00??000000?0000000
0??????001???????????????????00?000000000000000000?000000000000?0?0000001
00?
Protoceratops_andrewsi
000??0???0010000100000000??????000?0000000000?0100110000?000001000000000
0???????????????????000000000000?0000000000000000000000000000000000000
0000-
Zuniceratops_christopheri
111000???0??0??0?010?000?000?0?111100010211011?0??11?0???????0????????01?0
1000????1????????????????????11?1???1?0011011??001????1100?????????01?0??1???
Turanoceratops_tardabilis
?????????????????????0000??????1?1?00101?1?????????1?0???????????????????????
??1????????????????????????????????0???????1011???????????????????????????
Albertaceratops_nesmoi
?111?0???0??0??????01?1011100??11?1?0011211111112111???11001110010111011
110011111?000???00100010130300??1?1???1?11011?1???111??????????????????????0
0-
*Centrosaurus_apertus_*
011110???0??0??111001?11111101?1111000021111101112111110110011100101101
1110011111100000000100111200001111111111110111111111111111110111111111011
1111(0 1)00
Pachyrhinosaurus_lakustai
011110???0??0??111001?11111201011111????110?1?112?1111011001110010110101
1110011111??0???0?1001102110010111111?111011111111111?1?10??1111110111
??1(0 1)0-
*Chasmosaurus_belli_*
1110010101001000001001111111001111110000211111111211111111111101111121010
101001011101011100?00002132230?111111111101111111111111111210?1111111111
11111000
Chasmosaurus_russelli
1110010101001000001001111111001111110000211111111211111111111101111211010
101001011101011100?00002132230?11111??111011111111111111111210?1111111111
111?1000

Mojoceratops_perifania
1110010101001000001000011?1100011111011001111111101111111111110?111211011
0?011110??00003103030??????????????????1???????????????????????????????????0
00
Vagaceratops_irvinensis
1110011101001?0000100111111100011101?????111111112111?11111200111 0?211?01
1100000010100112011010021 23221?1111???1110111111 1?1111111?10?1111??11??1
1?1000
Kosmoceratops_richardsoni
1110011111001100001001111111100?11111011121111101111111111111200101112 1110
1110001001(01)102132111010021 32221????????11?011?111?1?11????????1??????????
???1000
Agujaceratops_mariscalensis
111001010100100000111?1111110001111011001111101111111??111?1011112?11??
1110?20111010?111?0???0????????111111???110?1111??1?111111210????111?11111?
?1000
Utahceratops_gettyi
11100101110?110000110?1111110001111111022111110111?111111111101111211110
111012011101121 2210?00013133030???1111?11101111111111111???1?10??????1??111
11?1000
Pentaceratops sternbergi
11100101110111000011011111110001111100112111110111111111111111101111221110
11101201110?1212210?000131330301111111111101111111111111111210?1111111111
?11??000
*Coahuilaceratops_magnacuerna_*
11100?1??10????00??1??11111110??1?11??11?1????????????????11??01?1??????01?1?
?2011101??1??????????????????????????1?0111111???11?????10???????????????1?00
*Anchiceratops_ornatus_*
1110011(01)1110110001001?11111100011111111111111101111111111112?01110?111
1011110011010012122 0(01)20000313303011111111?1?01?11???111111?10?1111?1
??111?110000
*Arrhinoceratops_brachyops_*
1110011??1?0100001?01?111?11000111 1?11111111110112 1111(01)?111??0111(01)?1
111011110011010?101110??000040040401111111 11?????????????11?????????????????
??????001
Bravoceratops_polyphemus
?1????????????????0????????11??????111011?1???1??111?????1?0???1?10?01??01?11?
2011101121211???110?1?????1111?????????????11??????????????????????????????110

Ojoceratops_fowleri
11??0??????????????0??????111??1??????????111????????????1120?101?????????1100
???101101110??00104004040????????111011?111???11??????0???????????????1?00
Torosaurus_latus
1110010??111???0010?1?1111111001111111(01)1121111101121111?(01)111111101110?1
12101011031201 0?1011100?1000400404011111111?1????????1111???1?10?????????
????????(01)00
Torosaurus_utahensis
????????????????????????????????11?1011211111011 2?1??1??11??01110?(01)121010
1103120101101111121010400404 0????????111?11111??1?111?11??????????????????1
???
Eotriceratops_xerinsularis
11100100?11011000??0??111111??011?111?1121?111?112???????11?1???1??????????
??????10?1?1???12?????????????????????????????????111????????????????????????1
Nedoceratops_hatcheri
11100100?1111110??0?1?111?1110011?1?10112?11110?12?1?11111111?101???021?1
1110311010?1011101????????????????111?????????????????1????????????????????????0
0
Triceratops_horridus
1110010??111111001001?11111110011111101121111101121111111111111101010?00211
001??????1011011101200104004040111111111110111111111111111211111111111111
11111(01)00
Triceratops_prorsus
11100100?111111001001?1111111001111110112111110112111101111111101010?00211
001??????101101110120010400404011111111111011111111111111111??1?????????????
?11(01)00
KUVP-16100*
?????????????????????11111?????1111101 11??11110111??11??11111??1???211101?10
1201110?????????0001311????1??11??
MNA V1747*
111001011101110000 11?111111100?11?110?11??11110?11??0111111110111122111 01
1101201110?1?12210?0001313303011??1???11101111111111 1?????????????????????
1?00
NMMNH P21098*
???111?????????????11????0????????????????
????100?10???????????????????????11????????????????10???????????????????

NMMNH P27468*
??11???????110???000?1???01?1???0
11?????????0?000?21211??
NMMNH P50000*
11100101110111000011?111111100?11111001121111101111 1????111???????????????
?????????????????????????????1???000